Low Energy Electron–Molecule Scattering Experiments and the Theory of Rotational Excitation

D. E. GOLDEN

Behlen Laboratory of Physics, University of Nebraska, Lincoln, Nebraska 68508

NEAL F. LANE*

Department of Physics, Rice University, Houston, Texas 77001

A. TEMKIN

NASA-Goddard Space Flight Center, Greenbelt, Maryland 20771

E. GERJUOY†

Department of Physics, University of Pittsburgh, Pittsburgh, Pennsylvania 15213

The various experimental techniques used to obtain differential, total, and momentum-transfer electron–molecule scattering cross sections at low electron energies are reviewed, and observations are compared with theory, especially with theoretical calculations of rotational excitation cross sections for slow electrons incident on homonuclear diatomic molecules. A detailed discussion of the theory of rotational excitation by slow electrons is given, with particular attention to the merits and deficiencies of recent attempts to improve on the lowest-order Born approximation predictions, via the so-called rotational close coupling and adiabatic-nuclei approximations.

CONTENTS

* Alfred P. Sloan Fellow. Supported in part by the U.S. Atomic Energy Commission.

† Supported in part by the Advanced Research Projects Agency under Contract No. DA-31-124-ARO-D-440 and by The National Aeronautics and Space Administration under Contract No. NGL-39-011-035.

1. INTRODUCTION ‡

Measurements of various electron scattering cross sections and related quantities (e.g., energy loss rates) have been carried out for approximately the past seventy years.[1] Reasonably successful theories of some of these cross sections have been proposed for very nearly the same length of time.[2] As electron collision physics has evolved, it has become apparent that the low-energy domain (which we will define to be the range of incident electron energies below the ionization threshold, e.g., from 0 to roughly 10 eV) is extremely

‡ This review is based on invited papers delivered individually by D. E. Golden, Neal F. Lane, and A. Temkin at The American Physical Society Division of Electron and Atomic Physics Symposium "Electron-Molecule Scattering", chaired by E. Gerjuoy, Washington, D.C., April 27, 1970. Each of the four authors of this review has read all four chapters, and is in general agreement with their contents. However, each author has been primarily responsible for a single section, as follows: Sec. 2: Low Energy Electron-Molecule Scattering Experiments, D. E. Golden; Sec. 3: Close Coupling Calculations of Elastic and Rotational Excitation Cross Sections for Electron–H_2 Collisions, Neal F. Lane; Sec. 4: Development of Fixed-Nuclei Approximations of Electron–Molecule Scattering and the Theory of Rotational Excitation, A. Temkin; brief overall Introduction, Sec. 1, E. Gerjuoy, who also has done the editing necessary to ensure consistency and no redundancy between the main Secs. 2–4.

[1] Kerwin, Marmet, and Carette (1969) state "Lenard (1903) appears to have been the first to bombard atoms with beams of low-energy electrons". Brode (1933) refers to even earlier electron collision measurements by Lenard.

[2] Cf., e.g., J. J. Thomson (1912), whose purely classical theory of ionization is closely related to the recently widely employed and often very successful classical binary encounter theory of Gryzinski (1965), whose theory in turn can be shown to be closely related to the quantum mechanical Born approximation [Stabler, 1964; Garcia, 1967; Vriens, 1969].

interesting, both experimentally and theoretically. In particular, there has been a continuing attempt—dating from the first really quantitative measurements, nearly fifty years ago[3]—to bring experiment and theory into agreement for the collisions of low-energy electrons with molecules, especially in the simplest circumstance that the target molecules are homonuclear and diatomic, e.g., H_2 or N_2.

Modern experimental techniques for obtaining low-energy electron–molecule collision cross sections are reviewed in Sec. 2 below, which also summarizes[4] much of the data for the atmospheric gases. The reproducibility of recent measurements by any one group, and the agreement between observations by different groups, are sufficiently impressive to justify the belief that most experimental low-energy electron–molecule cross sections now are acceptably reliable. Unfortunately, *ab initio* (i.e., starting from the Schrödinger equation, without incorporation of empirical information or adjustable parameters) theoretical prediction of most observed electron–molecule cross sections at incident energies below the ionization threshold still is impractically expensive and arduous with the best available high-speed computers. Of course, *ab initio* prediction of low-energy electron–atom collision cross sections is not yet practical either; but for collisions with not-too-complex target atoms at incident electron energies not too close to the ionization threshold, i.e., for collisions involving only a moderate number of open (energetically accessible) collision channels, the possibility of soon having codes which will routinely and practicably predict such electron–atom cross sections is reasonably promising. The difficulty with electron–molecule collisions is that even when the incident energy is capable of exciting merely a few electronic levels, there usually are a very large number of open channels, corresponding to the various rotational and vibrational levels which are energetically accessible. To keep the number of open channels small in electron–molecule collisions, the incident energy must be very low indeed by electron–atom collision standards; in fact, the incident energy must be so low that (with very few exceptions, surely) electron–atom collisions would be elastic and accurately describable by effective range theory.

The simplest electron–molecule collisions (other than purely elastic collisions) involve target molecules which are homonuclear and diatomic, at incident energies too low for vibrational excitation, though large enough for rotational excitation. As a matter of fact, for rotational excitation under these circumstances, there exists a first-order theory which is much more successful than any first-order theory of electron–atom excitation at low energies. To be specific, it was shown about fifteen years ago (Gerjuoy and Stein, 1955a, 1955b) that at incident energies just above the excitation threshold, the cross section for rotational excitation of homonuclear diatomic molecules by electrons depends solely on the molecular quadrupole moment, and is almost trivially correctly obtainable in closed form using the Born approximation. As the incident energy increases from threshold, the Born approximation is decreasingly valid, and the rotational excitation cross section commences to depend in a complicated manner on more collision parameters (e.g., on the molecular polarizability) than merely the quadrupole moment. The, at first sight, surprising conclusion that in rotational excitation of homonuclear diatomic molecules by electrons the Born approximation is best at the lowest energies is understandable from the fact that the electron–molecule interaction has a long-range tail, proportional to the molecular quadrupole moment Q and to r^{-3}, with r the distance between the incident electron and the molecular center; it then can be argued (Gerjuoy and Stein, 1955a) that as the incident wave length increases, the principal contribution to the matrix element for rotational excitation comes from increasingly large distances, where the ratio of the interaction energy to the incident kinetic energy approaches zero, therewith satisfying a customarily cited criterion for the validity of the Born approximation. This argument also explains the result that the rotational excitation cross section near threshold depends only on Q.

Consequently, the main theoretical interest in rotational excitation by electrons is to develop methods for correctly predicting observed cross sections as the energy increases from threshold, and departures from the simple Gerjuoy–Stein formulas develop. Sections 3 and 4 below review the most recent progress in this regard. In particular, Sec. 3 reviews results obtained in what may be termed the rotational close coupling approximation, while Sec. 4 examines the so-called fixed-nuclei approximation for elastic scattering, and its so-called "adiabatic-nuclei" counterpart for rotational excitation. The close-coupling approximation method [Burke and Smith, 1962] has been applied with varying degrees of success to several electron–atom problems, and its evolution is one of the reasons for our previous assertion that routine prediction of low-energy electron-atom cross sections soon may be practical. The method may be described in three steps: (i) Expansion of the total wavefunction describing the collision in terms of the complete set of target states,[5]

[3] References to the early experimental work on electron–molecule collisions are given by Massey and Burhop (1952), pp. 207–209, and by Brode (1933); judging by these sources the first reasonably believable measurements of such collisions were performed by Ramsauer (1921), and by Townsend and Bailey (1922).

[4] Other recent summaries of low-energy electron–molecule collision experiments, along with extensive references to the literature, include Massey, Burhop, and Gilbody (1969); McDaniel (1964); Phelps (1967, 1968); Varney and Fisher (1968). Primarily bibliographic compilations, not always entirely overlapping, include Takayanagi (1969); Hochstim (1969); Kieffer (1967); Chamberlain and Kieffer (1970).

[5] Close-coupling expansions in terms of so-called pseudostates (Damburg and Karule, 1967), which are designedly chosen different from the actual target states, also have been employed (Burke and Geltman, 1970).

including antisymmetrization with respect to interchange of all electrons, incident as well as target; the coefficients in such an expansion then may be interpreted as continuum electron orbitals, and must satisfy an infinity of coupled partial integro-differential equations. (ii) Next these continuum orbitals are expanded in terms of spherical harmonics ("partial wave expansion") resulting in an infinity of coupled ordinary integro-differential equations for the radial parts of the continuum orbitals. (iii) Finally, one makes the "close-coupling approximation" of truncating this last infinite set of equations, in order to make tractable the task of finding solutions satisfying appropriate asymptotic conditions. The fixed-nuclei approximation starts from a somewhat less fundamental point of view than the close-coupling method [which in principle would be exact if truncation were not necessary], but within its framework can be carried out very consistently; the basic idea is to replace the actual molecule by one in which the nuclei are fixed during the entire collision process, an approximation crudely defensible whenever the incident electron speed is large compared to the nuclear rotational speed [a criterion requiring merely that incident electron energies exceed 10^{-4} eV, for all electron–molecule collisions]. In this way, one obtains elastic scattering amplitudes, which then can be employed in a so-called "adiabatic-nuclei" approximation (again based on the fact that the incident electron speed is large compared to the nuclear rotational speed) to yield rotational excitation cross sections by simple quadratures. A perhaps more accurate criterion might be that the collision time is small compared to the molecular rotational period; however, the collision time is difficult to pin down without completely solving the problem. The criterion for the validity of the adiabatic-nuclei approximation is discussed further in Sec. 4; here it suffices to say that the incident energies at which the adiabatic-nuclei approximation is valid probably are larger than 10^{-4} eV.

Especially when the possibility of electron exchange is taken into account, either of the aforementioned approximations is considerably more complicated to carry out than the very simple Gerjuoy–Stein Born approximation, wherein electron exchange was wholly ignored. Unfortunately, it appears that these refinements are needed at energies quite close to threshold [in e^-–H_2 collisions, at energies merely seven hundredths of a volt above threshold (Chang, 1970), i.e., below the threshold for opening a second rotational excitation channel], if detailed agreement between theory and experiment is to be obtained. At the present time, only e^-–H_2 collisions have been studied sufficiently carefully both experimentally and theoretically to warrant any conclusions concerning the utility of these fixed-nuclei and close-coupling approximations in rotational excitation. In e^-–H_2 collisions, however, it does seem that either the close-coupling or the adiabatic-nuclei approximation is able to account for the observed rotational excitation cross sections at energies up to a few volts above threshold, and that the adiabatic-nuclei method involves rather less computation than does the rotational close-coupling method.

The foregoing remarks are amplified, elucidated and illustrated in Secs. 2–4 below. Sections 3 and 4, on the theory of rotational excitation by slow electrons, may be compared with a very recent review of the same subject by Takayanagi and Itikawa (1970), who also give extensive references to the literature. It is worth mentioning that Secs. 3 and 4, being concerned solely with homonuclear diatomic molecules, do not consider rotational excitation of molecules possessing a permanent dipole moment, for which there also is a successful first order theory at low incident energies, due to Altshuler (1957), who employed the Born approximation together with an adiabatic-nuclei approximation. For more recent theoretical treatments of electron scattering by polar molecules, see Takayanagi (1967); Tagayanagi and Itikawa (1968); Itikawa and Takayanagi (1969a); Itikawa (1967, 1969); Turner, Anderson, and Fox (1968); Garrett, Turner, and Anderson (1970); Bottcher (1970, 1971); Crawford (1971); Garrett (1971). For swarm data in a large variety of polar molecules, mostly organic and distinctly polyatomic, along with a summary of much of the relevant literature, see Christophorou and Christodoulides (1969).

2. Low-Energy Electron–Molecule Scattering Experiments

Although some reference will be made to older work, in general this chapter concentrates on the more modern measurements of electron–molecule scattering at energies below ionization, particularly in the atmospheric gases. Because hydrogen is the simplest molecular gas from a theoretical standpoint, and especially because Secs. 3 and 4 below are almost entirely concerned with e^-–H_2 collisions, these collisions will receive the most attention in this chapter.

2.1 Basic Experimental Procedures

There are three classes of measurements which can be performed. Most desirable, of course, would be a set of measurements of the differential cross section as a function of incoming and outgoing energy and angle. From such a set of measurements, one can directly obtain either the total cross section or the momentum-transfer cross section. In principle, at least, a direct measurement of the differential cross section is straightforward. All one need do is scatter a monoenergetic parallel electron beam by a monoenergetic line gas target; one then studies the scattered electrons arriving at a detector of infinite angular resolution as a function of angle, and as a function of incoming and outgoing energy. Such an arrangement is illustrated schematically in Fig. 1. In practice, the problems associated with making a low-energy quasimonoenergetic electron beam and a quasiline gas target, together with detecting the

scattered electrons at even some finite angular resolution, have proven to be somewhat difficult. The problems of unknown or at best variable detection efficiency arising from finite angular resolution can be, to a certain extent, overcome by a total scattering measurement. However, the problems associated with finite energy resolution become more serious as one goes to lower and lower energies. Ultimately, the problem of space charge (leading to loss of signal at very low energies) makes it impossible to measure scattering cross sections directly. In any case, as the energy is lowered, a measurement of scattering cross section as a point function of energy gradually becomes a measurement of the average value of the product of the cross section and collisional relative velocity, divided by the average value of the relative velocity. Thus at sufficiently low energies even a so-called direct measurement ends up with the problem of unfolding the desired cross section for monoenergetic particles from measurements averaged over the energy distribution functions of the colliding particles.

The direct measurement of electron scattering cross sections, both total and differential, was begun by Ramsauer in the early years of this century.[6] In these and subsequent measurements[7] a magnetic momentum selector was used to define the electron beam energy; then the beam was allowed to interact with a gas contained in a scattering cell, and the attenuation of the electron beam current was measured as a function of the gas density in the scattering cell at a particular electron energy and (in some cases) scattering angle. The arrangement for such measurements is shown very schematically in Fig. 2. Since the logarithm of the attenuated current is proportional to the total scattering cross section and the pressure, an absolute cross section measurement depends upon an absolute pressure measurement, usually at pressures below about 100μ.

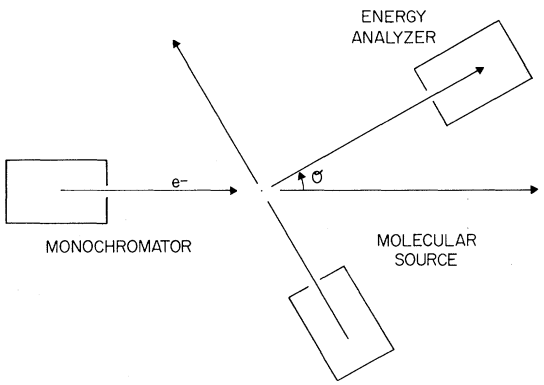

FIG. 1. A desirable experimental arrangement for a differential scattering cross section measurement.

[6] For total electron–molecule scattering see, e.g., Ramsauer and Kollath (1930); for differential electron–molecule scattering see, e.g., Ramsauer and Kollath (1932).

[7] For a discussion of the modern application of the Ramsauer technique to precise total electron-atom or molecule scattering cross section measurements, see Golden and Bandel (1965).

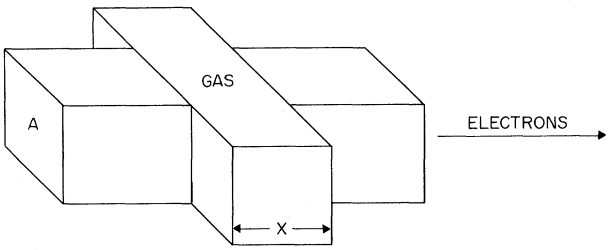

FIG. 2. Interaction region geometry. The incident electron beam has area A.

In the most recent measurements of this general nature (Golden, Bandel, and Salerno, 1966; Golden and Bandel, 1966; Golden, 1966a; Salop and Nakano, 1970), cross section measurements have been limited to electron energies greater than 100 meV, with an estimated probable error of $\pm 3\%$, arising mainly in the pressure measurement.[8]

Conversely, one may study the neutrals instead of the electrons. In such a case one need not measure the absolute neutral density, but rather one must measure the absolute value of electron current; obviously this is an advantage. However, in order to do such an experiment, one needs a molecular beam in addition to the electron beam, and hence one needs a method of measuring relative neutral fluxes at least. The molecular beam sidesteps the problem of absolute pressure measurement and allows the measurement of cross sections of atoms or molecules not normally available as gases, but at the same time introduces another problem, that of further loss of signal. For substances which are normally gases, the achievable beam density usually is at least 100 times less[9] than the corresponding gas density used in a beam–gas cell experiment, and can be as much as 10^6 times less[10] for substances made by dissociation. Thus the beam–beam experiments have usually been limited to energies greater than about 500 meV with an estimated probable error of about ± 20–30% (Sunshine, Aubrey, and Bederson, 1967). The difficulties associated with direct measurement of low-energy electron scattering cross sections has led to the re-emergence of the so-called indirect methods of cross section measurement, wherein the desired cross section is extracted from the data only after a fairly complicated analysis. The oldest of these methods, which determines the momentum-transfer cross section[11] from measurements of transport properties of electron swarms, was pioneered by Townsend (1914). In this

[8] Particular difficulties associated with the O_2 measurements have led Salop and Nakano (1970) to estimate their error to lie between ± 8 and $\pm 10\%$.

[9] See, for example, Ehrhardt, Langhans, Linder, and Taylor (1968).

[10] See, for example, Smith (1955).

[11] For a discussion of the modern application of the swarm technique see, for example, Crompton (1970). For a definition of the momentum-transfer cross section and a discussion of its significance in transport processes, see Massey and Burhop (1952), pp. 15–20.

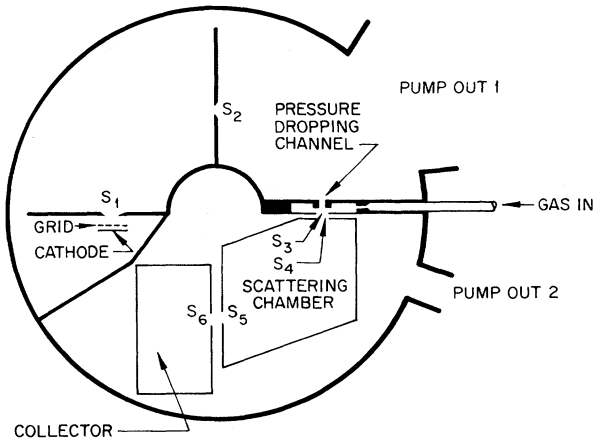

FIG. 3. Schematic arrangement of a modified Ramsauer apparatus for the measurement of total scattering cross section, from Golden and Bandel (1965).

chapter, remarks concerning indirect methods will be restricted to cross section determinations from these so-called "swarm" experiments,[11] since these data thus far have yielded much more precise information than other types of indirect measurements, and have done so for the largest variety of gases. Usually measured are the drift velocity and the ratio of the diffusion coefficient to mobility, as functions of the ratio of electric field strength E to density N. The pioneering work on the numerical solution of the ensuing Boltzmann equation to find the momentum-transfer cross section was done by Frost and Phelps (1962). The use of modern techniques in the measurement of both the drift velocity, v_d, and the ratio of diffusion coefficient to mobility, D/μ, such as employed by Crompton, Elford, and Jory (1967), has yielded measurements of these quantities with quoted accuracies of $\pm 1\%$ over a wide range of values of E/N. At the higher pressures used in swarm experiments, the principle source of error is the pressure measurement, but this error can be made less than 1%. For collisions with atoms at energies below the excitation threshold, the method applied by Crompton and others is to use an assumed cross section as a function of energy to calculate both v_d and D/μ as a function of the ratio of electric field strength to density, E/N. Then the cross section function is varied until the computed values of v_d and D/μ are consistent with the corresponding measured values. This has resulted (Crompton, Elford, and Jory, 1967) in a stated error of $\pm 2\%$ for electron–helium scattering in a range of energies from 10 meV to 3 eV.[12]

Because of inelastic effects, for molecular gases the same kind of analysis of transport data as was used for the atomic gases cannot be used to unfold the cross section. However, if all but one inelastic cross section is known accurately, the remaining inelastic cross section can be determined, and the analysis of the data near threshold is most precise. Moreover, if the only significant inelastic losses are due to one type of excitation process (such as rotational excitation), swarm methods can be used to normalize the cross sections measured by a beam experiment; alternatively, if the cross sections have been calculated from theory, both the theory and the physical parameters used in the theory (such as electric dipole and quadrupole moments) can be checked with the results of swarm experiments. The momentum-transfer cross section can be obtained with reasonable accuracy at all energies, provided the inelastic collision frequency is small compared to the elastic collision frequency. Crompton, Gibson, and McIntosh (1969) have estimated the error in their momentum-transfer cross section determinations in hydrogen to be $\pm 5\%$.[13] Modern differential scattering cross section measurements still are fragmentary but, hopefully, more data soon will be forthcoming.

2.2 Modern Experimental Methods

2.21 Modified Ramsauer Technique

Figure 3 shows a schematic diagram of an apparatus used by Golden and Bandel (1965) to make total cross section measurements. More recently this apparatus has been used by Salop and Nakano (1970). The apparatus is very similar to that used by Ramsauer and Kollath (1930), the major modification being the provision here for differential pumping. Briefly, the electrons from an oxide coated cathode, or (in the case of oxygen) a thoriated iridium filament, are momentum selected by the combination of the three slits, S_1, S_2, S_3, and a uniform magnetic field applied perpendicular to the plane of the drawing. The electrons are then allowed to interact with the gas to be studied in the scattering cell, and the transmitted electron signal is studied as a function of gas density in the scattering region at a particular value of electron energy. If it is assumed that a current of electrons $I_{c0}+I_{s0}=I_0$ enters the scattering region, the current reaching the collector is given by

$$I_c(\epsilon)=I_{c0}(\epsilon)\ \exp\left[-\sigma_t(\epsilon)Nx\right], \qquad (2.1)$$

where I_{c0} is that part of the current entering the scattering region which would reach the collector in the absence of scattering, $\sigma_t(\epsilon)$ is the total cross section, N is the gas density, x is the path length of the electron beam through the scattering chamber, and ϵ is the electron energy. The current reaching the scattering chamber walls is given by

$$I_s=I_{s0}+I_{c0}\left[1-\exp\left(-\sigma_t Nx\right)\right] \qquad (2.2)$$

where I_{s0} is that part of the current entering the scattering chamber which would reach the scattering

[12] It should be noted that attempts to compare total and momentum-transfer cross sections through a phase-shift analysis of the data show that even in the case of He the total and momentum-transfer cross sections do not agree to better than about 10%. For this type of analysis see, for example, Golden (1966b), Bransden and McDowell (1969).

[13] For a comparison between the results in H_2 and D_2 see Engelhardt and Phelps (1963); for N_2, see Engelhardt, Phelps, and Risk (1964); for momentum-transfer cross section determinations in O_2, CO, and CO_2, see Hake and Phelps (1967).

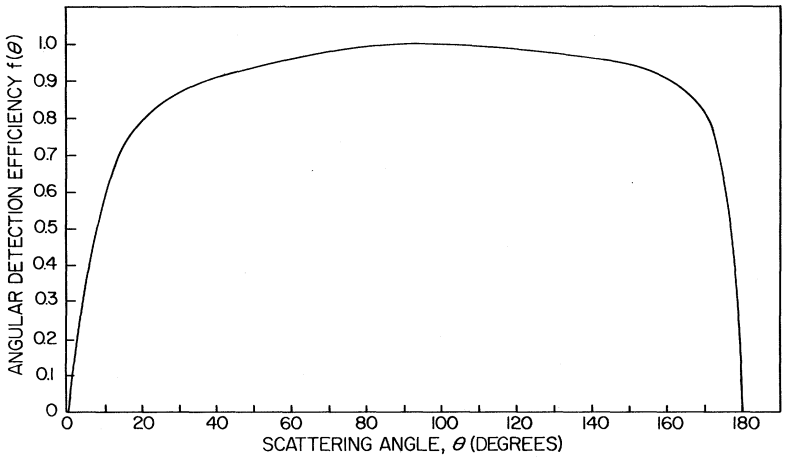

FIG. 4. Approximate angular detection efficiency function of the modified Ramsauer apparatus of Fig. 3, from Golden and Bandel (1965).

chamber walls in the absence of scattering. Then we have

$$\ln\left[(I_c+I_s)/I_c\right]=\ln\left[(I_{c0}+I_{s0})/I_{c0}\right]+\sigma_t N x. \quad (2.3)$$

From Eq. (2.3) the total cross section is directly determined by measuring the slope of a plot of the left hand side vs N at constant ϵ. In this kind of selector, two parameters define the electron energy. One is the magnetic field strength and the other is the accelerating voltage. This coupling of the energy to two experimental parameters leads to the fact that the electron energy is not easily continuously variable. The energy resolution of this type of apparatus is roughly given by

$$\Re\equiv\epsilon/\Delta\epsilon\simeq r_a/2\Delta w \quad (2.4)$$

where $\Delta\epsilon$ is the electron energy spread passed by the slit system, r_a is the mean radius of the apparatus, and Δw is the slit width. Since the energy resolution is a constant, the energy spread passed is a function of the energy. Thus the study of resonance effects is quite a tedious affair. However, there is an advantage with regard to changes in accelerating potential due to interactions between the cathode and background gas [Golden, Bandel, and Salerno 1966]. For a given value of magnetic field strength, only one value of electron energy will be transmitted regardless of the applied accelerating voltage. Figure 4 shows the angular detection efficiency for this kind of a transmission experiment to measure total scattering cross section. This function has been calculated for a rectangular geometry without a magnetic field, and as such is only an approximation (although a pessimistic one) to the true situation in a Ramsauer apparatus.[7] If we define the angular resolution as the angle at which 50% of the scattering events are detected, the apparatus has an 8° resolution for forward scattering, and a 2° resolution for backward scattering. In order to estimate how much of the total cross section is measured, this function must be multiplied by the differential cross section and the element of solid angle, and then integrated over the angle. Hence the lack of detection at zero and 180° is somewhat minimized. Estimates based upon calculated differential cross sections for hydrogen or helium, using this geometrically derived function, give the result that the experiment measures about 99% of the total scattering cross section.

2.22 *Molecular Beam Recoil Technique*

Figure 5 shows the schematic arrangement for the atomic or molecular beam recoil experiment of Sunshine, Aubrey, and Bederson (1967). The gas from the source goes through some collimating slits and then is cross fired with a pulsed electron beam. The transmitted atoms or molecules are detected by a phase-sensitive detector locked to the pulse frequency of the electron beam. The output of the phase-sensitive detector is connected to the input of a voltage to frequency converter, the output of which is connected to a scaler timer for signal enhancement. Sunshine, Aubrey, and Bederson (1967) show that for electron–molecule scattering the total cross section σ_t is given by

$$\sigma_t=1.064(He\bar{v}/i)(S/I), \quad (2.5)$$

where H is the common dimension of electron and neutral beams at their intersection, i/e is the number of electrons per second in the interaction region, $\bar{v}$ is the most probable velocity of the neutral beam in the source, and S/I is the ratio of the measured scattering signal to the total beam signal. This equation takes into account the distribution of molecular velocities, including corrections for the transit time of the neutral beam. For molecular oxygen, the angular resolution of this apparatus using the 50% criterion ranges from about 18.5° at 1 eV to 11.5° at 12 eV.

2.23 *Electron Swarm Techniques*

Figure 6 shows the chamber used by Crompton, Elford, and Gascoigne (1965) to measure the ratio of diffusion coefficient to mobility as a function of the ratio of electric field strength to gas density. Electrons enter the chamber through the small hole in the cathode,

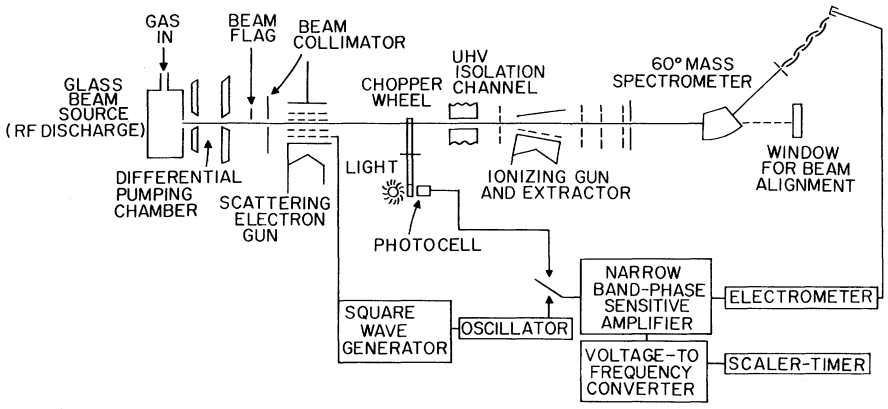

FIG. 5. Schematic arrangement of an atomic or molecular beam recoil experiment from Sunshine, Aubrey, and Bederson (1967).

and drift and diffuse under the influence of a uniform electric field towards the anode. The anode is divided into a disk and an annulus, and the ratio of electron currents to the two parts of the anode is measured. This ratio is related in a complicated way to the ratio of diffusion coefficient to mobility, D/μ. Figure 7 shows a slightly different chamber employed by the same authors; this one is used to measure the drift velocity as a function of the ratio of electric field strength to density. Here the time required for a pulse of electrons to go from one electrical shutter through the other to the collector is measured, and this is related straightforwardly to the drift velocity. The diffusion equation has been solved for the electron drift, subject to the boundary conditions that the density is zero at the cathode and anode except for a point electron source at the cathode [Huxley, 1940].[14] The particular form of the Boltzmann equation given by Frost and Phelps (1962), which was derived by Holstein (1946) and Margenau (1946) to include the effect of the molecular energy distribution function, is

$$\tfrac{1}{3}(E^2e^2)\frac{d}{d\epsilon}\left(\frac{\epsilon}{N\sigma_m(\epsilon)}\frac{df(\epsilon)}{d\epsilon}\right)+\frac{2m}{M}\frac{d}{d\epsilon}[\epsilon^2N\sigma_m(\epsilon)f(\epsilon)]$$
$$+\frac{2mkT}{M}\frac{d}{d\epsilon}\left(\epsilon^2N\sigma_m(\epsilon)\frac{df(\epsilon)}{d\epsilon}\right)$$
$$+\sum_j[(\epsilon+\epsilon_j)f(\epsilon+\epsilon_j)N\sigma_j(\epsilon+\epsilon_j)-\epsilon f(\epsilon)N\sigma_j(\epsilon)]$$
$$+\sum_j[(\epsilon-\epsilon_j)f(\epsilon-\epsilon_j)N\sigma_{-j}(\epsilon-\epsilon_j)-\epsilon f(\epsilon)N\sigma_{-j}(\epsilon)]=0 \tag{2.6}$$

with the distribution function normalization

$$\int_0^\infty \epsilon^{1/2}f(\epsilon)\,d\epsilon=1. \tag{2.7}$$

Equation (2.6) may be solved for the steady state distribution function $f(\epsilon)$ of a swarm of electrons drifting and diffusing through a gas at temperature T under the influence of a uniform electric field E. In this equation N is the gas density; $\sigma_m(\epsilon)$ is the momentum-transfer cross section; $\sigma_j(\epsilon)$ is a rotational, vibrational, or electronic excitation cross section of excitation energy ϵ_j; $\sigma_{-j}(\epsilon)$ is the cross section for collisions of the second kind in which an excitation energy ϵ_j is gained from the molecule. The symbol e is electron charge;

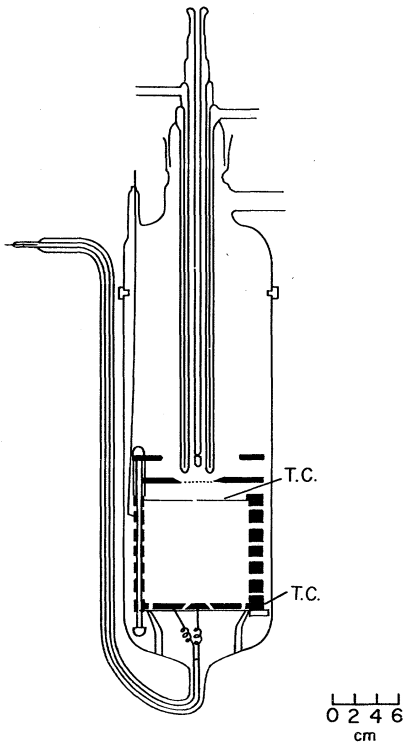

FIG. 6. Schematic arrangement of a Drift tube used to measure the ratio of diffusion coefficient to mobility, from Crompton, Elford, and Gascoigne (1965); TC denotes "thermocouple".

[14] A slightly different solution was obtained by Huxley and Crompton (1955), by changing the boundary conditions of the diffusion equation. When this was done, the resulting equation was found to agree closely with the experimental results.

m is the electron mass; M is the molecular mass, and k is the Boltzmann constant.[15]

It would be possible to measure $f(\epsilon)$ directly, and thus to solve Eq. (2.6) for the cross sections by varying trial sets of cross sections as a function of ϵ until Eq. (2.6) is satisfied for the known $f(\epsilon)$. However, electron energy distribution functions have only been measured directly in a few cases (Roberts and Burch, 1966; Golden and Nakano, 1967). The procedure that usually has been adopted is to compare experimental and calculated values of the electron drift velocity and diffusion coefficients as functions of the ratio of electric field strength to density. These quantities are given by

$$v_d = -\tfrac{1}{3}e\left(\frac{2}{m}\right)^{1/2}\left(\frac{E}{N}\right)\int_0^\infty \frac{\epsilon}{\sigma_m(\epsilon)}\frac{df(\epsilon)}{d\epsilon}\,d\epsilon, \quad (2.8)$$

and

$$\frac{De}{\mu} = \int_0^\infty \frac{\epsilon f(\epsilon)\,d\epsilon}{\sigma_m(\epsilon)} \Big/ \int_0^\infty \frac{\epsilon}{\sigma_m(\epsilon)}\frac{df(\epsilon)}{d\epsilon}\,d\epsilon. \quad (2.9)$$

Thus $f(\epsilon)$ is calculated from Eq. (2.6) for specified trial cross sections; then the right sides of Eqs. (2.8) and (2.9) are computed using the calculated $f(\epsilon)$ and the same trial $\sigma_m(\epsilon)$. The trial cross sections are varied until agreement for calculated and measured values of v_d, and De/μ is obtained within the experimental accuracies of these quantities.

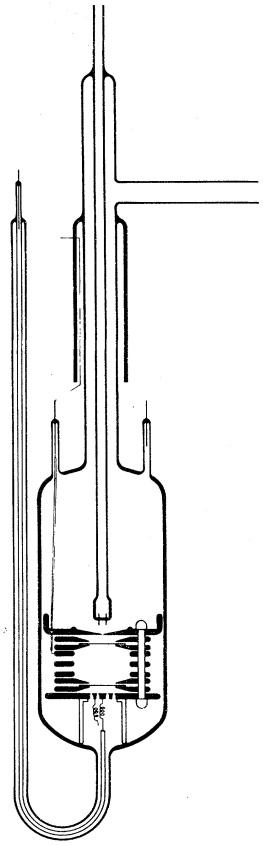

FIG. 7. Schematic arrangement of a Drift tube used to measure the drift velocity, from Crompton, Elford, and Gascoigne (1965).

In practice, the procedure which has just been described is useful mainly at lower energies, where only elastic scattering and at most one inelastic excitation is energetically possible. When only elastic scattering can occur, this swarm technique conveniently determines the momentum transfer cross section $\sigma_m(\epsilon)$, because the electron energies which make up a characteristic swarm and significantly contribute to the integrals of Eqs. (2.8) and (2.9) extend from zero to only about twice the mean energy. There may be many different cross section functions which would yield the correct transport integrals for a limited range of values of E/N (Margenau, 1946). However, when a wider range of values of E/N is used in conjunction with precise experimental results, a wider energy range of validity of the cross section as a function of energy will be obtained. In fact, definite limits can be obtained for the cross section's validity. In the case of only one inelastic process it is still possible to determine the cross section almost as accurately as in the case of elastic scattering, because only σ_m enters into the transport integrals [Eqs. (2.8) and (2.9)], while the inelastic cross section only affects the energy distribution function. However, when more than one inelastic process is important in the determination of the energy distribution, the situation becomes less clear. If only two inelastic processes are considered, with cross sections $\sigma_1(\epsilon)$, $\sigma_2(\epsilon)$ at threshold energies ϵ_1, ϵ_2 respectively (where $\epsilon_2 > \epsilon_1$), then at some energy between ϵ_1 and ϵ_2 neither $\sigma_1(\epsilon)$ nor $\sigma_2(\epsilon)$ can be uniquely determined from swarm data alone; above this energy, σ_1 cannot be uniquely determined unless σ_2 is known accurately from some other source. Furthermore, σ_2 can never be determined with a great deal of accuracy unless $\epsilon_2 \gg \epsilon_1$.

There are other methods of making direct cross section measurements, which have not been fully applied to either total or differential cross sections at low energies in an absolute way as yet, but which probably will be in the near future. However, they have been used to look at a number of elastic and inelastic effects, and therefore warrant some attention.

2.24 High Sensitivity Techniques

2.24a rpd *Technique.* Figure 8 shows an electron gun of the retarding potential difference type due to Schulz and Fox (1957). This was used in the first experiment which attempted to look at resonance effects in electron–atom scattering, by looking for the production of helium metastables as a function of electron energy in the vicinity of the threshold of the first triplet S level of He. An electron beam from the cathode is aligned and

[15] It should be noted that this form of the Boltzmann equation has neglected transverse spatial gradient terms in the distribution function. However, Lowke and Parker (1969) have shown that (despite this difficulty) calculations based on solutions of Eq. (2.6) agree with the experimentally obtained ratios of longitudinal and transverse diffusion coefficients to mobility.

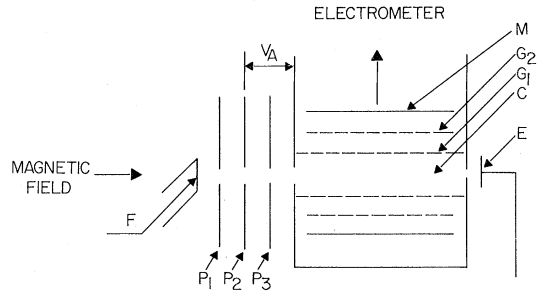

FIG. 8. Schematic arrangement of a retarding potential difference electron gun, from Schulz and Fox (1957). Here F is the filament; P_1, P_2, and P_3 are the three electrodes constituting the electron gun; C is the collision chamber; G_1 and G_2 are two concentric cylindrical grids; M is the gold-plated cylinder where electrons released by metastable atoms are measured; and E is the collector for electrons in the electron beam.

held together by a magnetic field pointed along the direction of the cathode-collector axis. A square wave retarding potential is applied to P_2, which serves as a dispersing element. Thus the ac current arriving at E in phase with the pulse applied to P_2 has, in principle, an energy width equal to the pulse height applied to P_2.[16] By proper choice of the potential on the transverse elements defining the interaction region, electrons which have lost a prescribed amount of energy may be trapped; thus the device can also serve as a sort of energy analyzer.[17] In practice this geometry has led to energy widths greater than about 100 meV, the reason being that the retarding potential works on solely the axial component of velocity, whereas the only limits on the allowable transverse velocity components are those given by the aperture dimensions and the applied magnetic field strength.[18]

2.24b *Electrostatic Monochromator-Analyzer Technique.* Figure 9 shows the schematic arrangement of the electrostatic monochromator–energy analyzer combination Simpson, Kuyatt, and Mielczarek used in their transmission experiments to study structured effects in electron scattering (Simpson 1964). This method of energy selection was first described by Hughes and Rojansky (1929). In this version, the lenses have cylindrical symmetry, and both monochromator and analyzer are spherical sections. In the monochromator, the electrons first are energy selected by the combination of the radial electrostatic field and the apertures, and then interact with the gas in the scattering cell; the transmitted electrons may be studied as a function of interaction energy and energy loss by means of another monochromator used to look at the transmitted electron energies. The resolution of this kind of monochromator is given by [compare Eq. (2.4)]

$$\mathcal{R} \equiv \epsilon/\Delta\epsilon \cong r_a/\Delta w_a, \tag{2.10}$$

where r_a now is the mean radius of the monochromator, and Δw_a is the aperture dimension. Since the energy resolution and the energy in this type of apparatus each are dependent upon only one parameter (namely and respectively the voltage between the spherical sections and the voltage on the scattering cell), the energy in the interaction region easily may be continuously varied. Thus resonance effects are easily studied. The gas cell may be replaced by a cross fired molecular beam, and either the monochromator or energy analyzer may be made movable so as to study the scattered electrons. This has been done most recently in the excellent experiments of Weingartshofer, Ehrhardt, Hermann, and Linder (1970) on electron–hydrogen molecule scattering, where both angular distribution and energy loss were observed.

2.3 Experimental Results

We shall review first experimental results in atmospheric gases other than hydrogen, deferring our discussion of e^-–H_2 collisions (wherein we examine rather small effects) to the end of this section. For the most part, we are concerned with measurements of total and momentum-transfer cross sections, performed via techniques described above. For a review of work prior to 1968, especially of rotational and vibrational excitation, covering H_2, N_2, O_2, CO, and CO_2, see Phelps (1968).

2.31 Total and Momentum-Transfer Cross Sections

2.31a *Nitrogen.* Figure 10 shows a total cross section measurement for N_2, done in a Ramsauer-type apparatus (Golden, 1966a). Also shown on the plot are the older measurements of Bruche (1927) and the semi-empirical calculations of Fisk (1936). Some discussion of Fisk's work (which included calculations of cross sections for O_2 and H_2) and its significance is given in Sec. 4 below. There is a broad peak in the measured total cross section at about 2.25 eV. The position of this peak is the same as the peak found by Schulz (1964) in a direct measurement of the cross section for vibrational excitation. Schulz's measurements give a peak total vibrational excitation cross section of about 5 Å^2 (roughly one-fifth the peak height seen on Fig. 10 disregarding the larger resonances). This result is consistent with the analysis of swarm data in N_2 performed by Englehardt, Phelps, and Risk (1964), shown on Fig. 11. However, the very large resonances (widths about 0.2 eV) which have first been observed by Schulz (1964), who also showed them to be elastic, cannot be resolved in the swarm measurements. These resonances are believed to be due to the temporary

[16] For a more complete discussion of the retarding potential difference method, see Fox, Hickam, Kjeldaas, and Grove (1951), and Fox, Hickam, and Grove (1953, 1955).

[17] For a discussion of the trapped electron method as applied to a retarding potential difference electron gun, see Schulz (1958, 1959).

[18] Recently this drawback has been overcome in a device operated at zero magnetic field; in fact an energy modulated electron spectrometer capable of energy resolution better than 0.01 eV has been demonstrated. For a description of this electron spectrometer, see Golden and Zecca (1971a). For the use of this spectrometer as applied to the study of resonance effects in e^-–He scattering, see Golden and Zecca (1970).

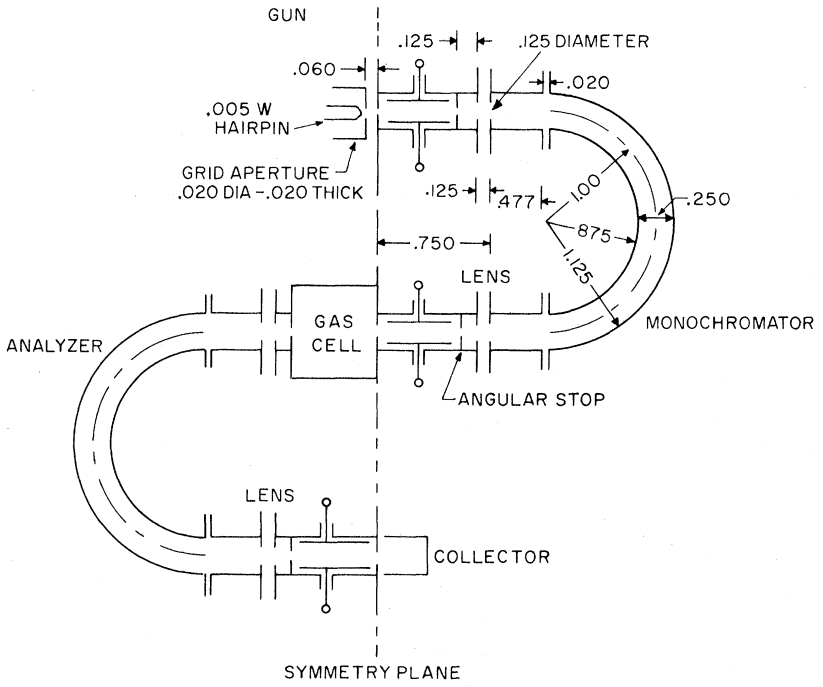

FIG. 9. Schematic arrangement of the electrostatic monochromator–energy analyzer, from Simpson (1964).

formation of N_2^- in the $^2\Pi_g$ state.[19] There also appear in Golden's (1966a) data some smaller structures at the lower electron energies which also may have been observed by Boness and Hasted (1966) in a transmission experiment using an electrostatic analyzer. Since no energy analysis was performed by Golden (1966a), it is not known whether these structures are elastic or not. Some preliminary measurements with a high energy resolution, energy modulated electron spectrometer[18] have also revealed these lower energy structures (Golden and Zecca 1971b), but as yet they have not been energy analyzed; thus whether they are elastic or inelastic or due to direct vibrational excitation must be decided by additional work. In any case, N_2 is a gas in which resonances play an important role in the scattering process, and a theoretical picture which attempts to explain the total scattering in N_2 should include provision for the formation of intermediate states of N_2^-. (Burke and Sinfailam, 1970; Krauss and Mies, 1970).

2.31b *Oxygen.* Figure 12 shows the very recently measured (Salop and Nakano, 1970) total cross sections in e^-–O_2 collisions. No large resonance effects are seen. The plot also shows the recent molecular beam recoil measurements of Sunshine, Aubrey, and Bederson (1967), the results of Bruche (1927), and the semiempirical calculations of Fisk (1936). Figure 13 shows swarm results for the momentum-transfer cross section and other inelastic cross sections in oxygen (Hake and Phelps, 1967). The agreement at the higher energies between the momentum-transfer cross section and the total cross section is very good.

[19] For the potential energy curve of this state of N_2^-, based on the measurements of Schulz (1964), see Gilmore (1965).

2.31c *Carbon Monoxide.* Figure 14 shows the momentum-transfer cross section in carbon monoxide (Hake and Phelps, 1967), which is a heteronuclear diatomic molecule, and therefore possesses a permanent electric dipole moment. Also shown on the plot are the Born approximation calculations of Altshuler (1957) for the momentum-transfer cross section, as well as the total cross section (Ramsauer and Kollath, 1931; Kollath, 1932). For the specific case of e^-–CO collisions, attempts to improve on first order Born approximation predictions of rotational and/or vibrational excitation cross sections include Takayanagi (1966), Itikawa and Takayanagi (1969b), and Itikawa (1970).

2.31d *Carbon Dioxide.* Figure 15 shows momentum-transfer cross sections in CO_2 (Hake and Phelps, 1967), along with other inelastic cross sections. Also shown on the plot are the total cross section measurements of Ramsauer and Kollath (1931) and Bruche (1927). As in the case of O_2, there is good agreement between momentum-transfer and total cross sections, especially at the higher energies. The peak at about 4 eV coincides with the maximum found by Schulz (unpublished) in the energy loss spectrum. It is also suggestive of the structure in N_2 at about 2.25 eV, which is resonant in character.

2.31e *Hydrogen.* Figure 16 shows a set of direct total cross section measurements in hydrogen and deuterium (Golden, Bandel, and Salerno 1966); the total cross sections in these two gases are identical on this scale. Also shown are the older measurements of Ramsauer and Kollath and the old semiempirical calculation of Fisk (1936). Detailed comparison of these measured e^-–H_2 cross sections with more recent theoretical calculations will be deferred to Secs. 3 and 4.

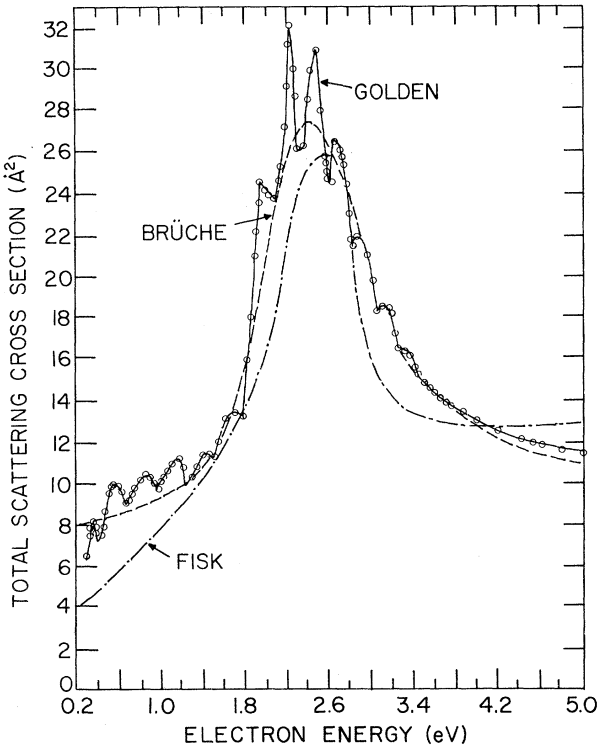

FIG. 10. Total scattering cross sections in square Angstroms for e^-–N_2, from Golden (1966a), Bruche (1927), and Fisk (1936).

Figure 17 shows the results for the momentum-transfer cross section in hydrogen. Here we have the calculations of Henry and Lane (1969), the swarm results of Engelhardt and Phelps (1963), and the swarm results of Crompton, Gibson, and McIntosh (1969). There is fairly good agreement between the calculations and the experiment (maximum disagreement with Henry and Lane is 40% at low energies). However, the significance of this comparison between experiment and theory in Fig. 17 is best evaluated in the light of the discussion in Secs. 3 and 4 below.

2.32 *Other Observations in Hydrogen*

We next shall review the smaller effects in hydrogen which can be seen with high sensitivity experiments. Many of these effects have been seen in other gases, but the discussion will be restricted to hydrogen.

2.32a *Resonances.* Figure 18 shows the results[20] of the transmission experiment of Kuyatt, Simpson, and Mielczarek (1966) in H_2, D_2 and HD. The transmitted current of electrons which have suffered no energy loss is plotted as a function of incident electron energy for the energy range 11–13 eV. Two series of bumps can be seen in each case, the observation being clearest in HD. The larger of the series has been shown to represent changes in cross section of about 2×10^{-18} cm², a factor of about 2.5×10^{-3} smaller than the elastic scattering at that energy.[20] These bumps are elastic resonances[21] due to the temporary formation of H_2^- in $^2\Sigma_g^+$ states at about 11 eV. Recently Weingartshofer, Ehrhardt, Hermann, and Linder (1970) have measured differential excitation functions and angular dependence of the scattered electrons for fixed incident energy and given decay channel, and have found an additional state of H_2^- at about 13.6 eV. The potential energy curves given by them for some of the H_2 states and H_2^- resonant states are shown in Fig. 19.

2.32b *Dissociative Attachment.* In the same energy regime an even smaller effect has been observed. Some of the structures in the dissociative attachment cross section are probably also due to the formation of temporary states of H_2^-. Figure 20 shows the dissociative attachment cross sections for electrons incident on H_2, HD, and D_2, measured by Rapp, Sharp, and Briglia

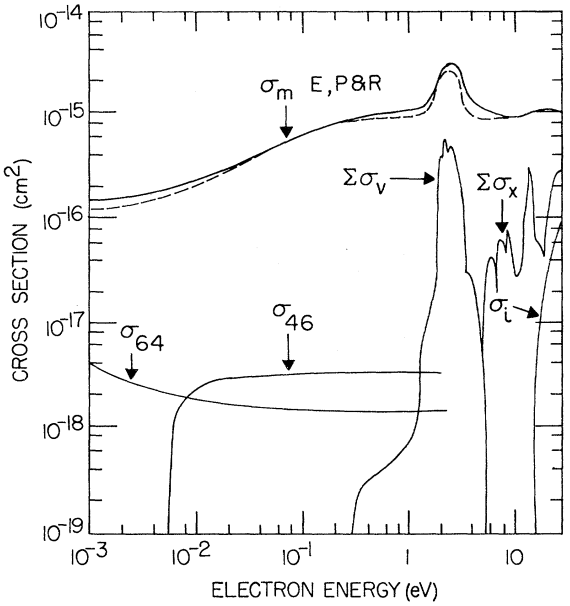

FIG. 11. Momentum-transfer, σ_m, and other inelastic cross sections for e^-–N_2, from Engelhardt, Phelps, and Risk (1964). The dashed σ_m curve indicates the results reported previously by Frost and Phelps (1962). To avoid confusion, only one rotational excitation curve is shown, namely σ_{46} from $j=4$ to $j=6$ calculated at 77°K from the Gerjuoy and Stein (1955a, 1955b) formulas using a quadrupole moment of 1.04 in atomic units; the corresponding deexcitation curve, from $j=6$ to $j=4$, is labeled σ_{64}. The curve labeled $\Sigma\sigma_v$ represents the total of all vibrational excitation cross sections to vibration levels $v=1-8$; the curve labeled $\Sigma\sigma_x$ represents the total of six various types of effective processes with thresholds between 5.0 and 14.0 eV. The ionization cross section, σ_i, represents the experimental results of Tate and Smith (1932).

[20] The stronger series of these resonances in H_2 was first observed by Kuyatt, Simpson, and Mielczarek (1964). The measurements were extended to D_2 by Golden and Bandel (1965b), who also gave quantitative information about the cross section changes in and out of the resonances.

[21] The spacings of these resonances in H_2 have been calculated by Taylor and Williams (1965), and agree moderately well with those shown in Fig. 18. See also Eliezer, Taylor, and Williams (1967).

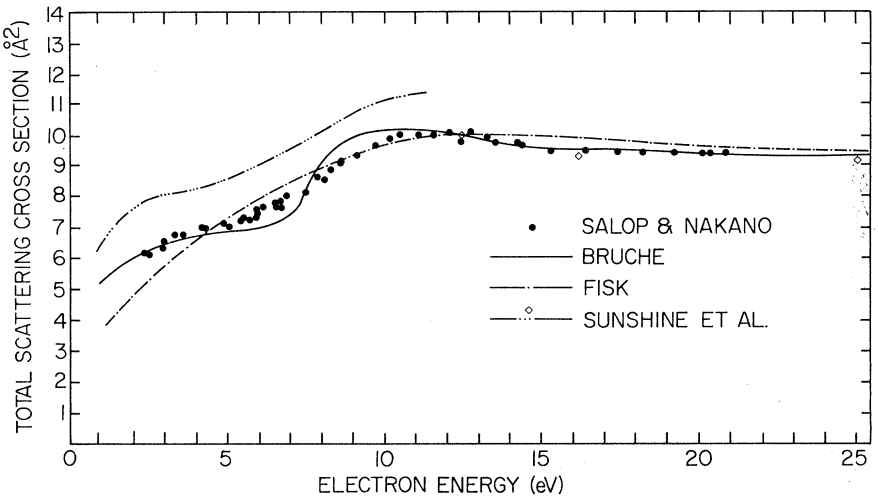

FIG. 12. Total scattering cross sections for e^-–O_2, from Salop and Nakano (1970); Sunshine, Aubrey, and Bederson (1967); Bruche (1927); and Fisk (1936).

(1965). The apparatus was essentially as described by Tate and Smith (1932), and similar to that used by Schulz and Fox (1957). The negative ion current was directly collected by one-half of a parallel plate capacitor, placed across the interaction region so that the incident electrons moved in the center of the capacitor and across its field. The lower energy portion of the H_2 curve in Fig. 20 is believed to be due to the formation of H^-, with the neutral H left in the ground state; the dissociative attachment presumably occurs via the $^2\Sigma_g^+$ repulsive state of H_2^-, and produces H^- ions having considerable kinetic energy. On the other hand, the upper peak in Fig. 20 is ascribed to H^- formation proceeding via a temporary excited state of H_2^- and leaving the neutral H in an excited state, so that very little kinetic energy remains to be shared between the outgoing H and H^-. The upper ($\sim$13.5 eV) H_2 peak in Fig. 20 is smaller than the elastic cross section at that energy by a factor of about 2.5×10^{-5}. In a more recent experiment employing essentially the same apparatus as Rapp, Sharp, and Briglia (1965), but with the addition of an electron trap which collects electrons that have undergone inelastic collisions,[17] Dowell and Sharp (1967) have found vibrational structure in the dissociative attachment cross section at the lower energy broad peaks of Fig. 20; this structure superimposed on Fig. 20 occurs at the same positions as the strong series of resonances found by Kuyatt, Simpson, and Mielczarek (1966). The existence of such structure seems to have been predicted by O'Malley (1966), and

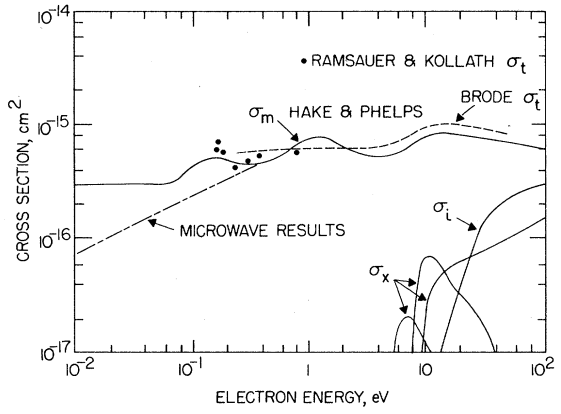

FIG. 13. Momentum-transfer σ_m and other inelastic cross sections for e^-–O_2, from Hake and Phelps (1967). The curve for σ_m labeled "microwave results" was derived from measurements by Mentzoni (1965) and by Veatch, Verdeyen, and Cohn (1966). Also shown are total cross section results σ_t by Brode (1933), dashed line; and by Ramsauer and Kollath (1930), points. The curves labeled σ_x denote various types of effective processes with threshold beginning at about 8.0 eV. The ionization cross section σ_i is taken from Tate and Smith (1932).

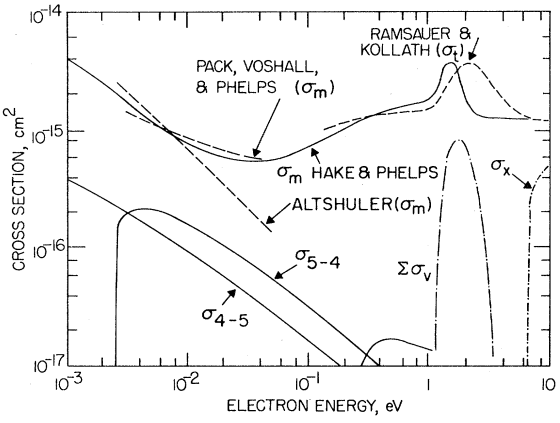

FIG. 14. Momentum-transfer, σ_m, and other inelastic cross sections for e^-–CO, from Hake and Phelps (1967). Also shown are values of σ_m from an earlier analysis of swarm data, by Pack, Voshall, and Phelps (1962), and theoretical estimates of σ_m, by Altshuler (1957). To avoid confusion, only one rotational excitation curve is shown, namely σ_{4-5} from $j=4$ to $j=5$; the corresponding deexcitation curve, from $j=5$ to $j=4$, is labeled σ_{5-4}. The curve labeled $\Sigma\sigma_v$ represents the sum of all energetically possible vibrational excitations from the ground state. The curve labeled σ_x is an electronic excitation cross section suggested by electron beam data. Measured values of the total cross section are denoted by σ_t.

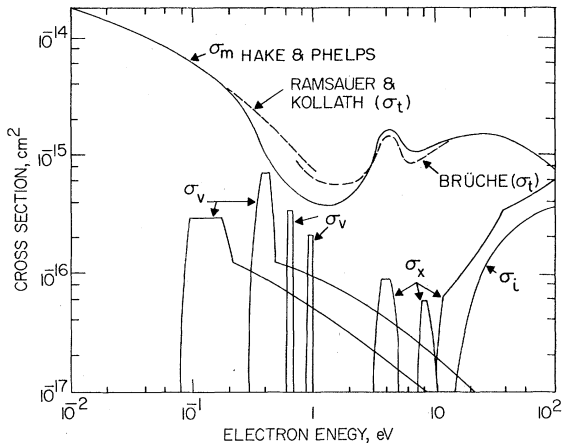

FIG. 15. Momentum-transfer σ_m and other inelastic cross sections for e^-–CO_2, from Hake and Phelps (1967). Various vibrational cross sections are labeled σ_v; various excitation processes are labeled σ_x; the ionization cross section is σ_i. Total cross sections are labeled σ_t.

there has been further theoretical work on this dissociative attachment problem by O'Malley and Taylor (1968).

Figure 21 shows a plot of the H^- ion current formed from electrons on H_2 as a function of electron energy at about 3.73 eV, as given by Schulz and Asundi (1965), using an apparatus similar to that employed by Dowell and Sharp (1967). In this lower electron energy range, the hydrogen atom comes off with essentially zero kinetic energy. The peak cross section has been estimated by Schulz and Asundi to be about 2×10^{-5} of the elastic cross section at that energy; they have postulated that this peak results from a resonant process, the process probably proceeding via the $^2\Sigma_u^+$ unstable ground state of H_2^-.[22] We shall make some comments in Sec. 4 concerning this "resonance".

2.32c *Vibrational and Rotational Excitation.* Several authors (Ehrhardt, Langhans, Linder, and Taylor, 1968; Crompton, Gibson, and McIntosh, 1969; Engelhardt and Phelps, 1963; Burrow and Schulz, 1969; Schulz, 1964) have measured the cross section for vibrational excitation by electrons on H_2, from the ground state to the first excited state ($v=0\rightarrow1$) for electron energies close to threshold (0.513 eV). All of the above authors have found an almost linear rise of cross section with energy near threshold. The indirect experiment of Crompton, Gibson, and McIntosh (1969) has found the lowest initial slope (0.11 Å^2/eV), while the direct measurements of Ehrhardt, Langhans, Linder, and Taylor (1968) have found 0.21 Å^2/eV [in agreement with the value given by Engelhardt and Phelps (1963) in another indirect experiment]. The most recent direct experiment using the trapped electron method (Burrow and Schulz, 1969) gives a slope of about 0.43 Å^2/eV, while the older direct experiment of Schulz (1964) gave an even larger slope (0.6 A^2/eV).[23]

Recently Crompton, Gibson, and Robertson (1970) have determined the threshold behavior of the cross section for vibrational excitation of H_2 by electrons from swarm data, using the apparatus of Crompton and McIntosh (1968). They found from drift velocity measurements that the power absorbed by rotational excitation in normal and parahydrogen were equal for 10^{-17} volt-cm^2 $\leq E/N \leq 26\times10^{-17}$ volt-cm^2. This is consistent with the proposition that, near threshold at least, the vibrational excitation cross section is the same for molecules in either the $j=0$ or $j=1$ rotational states. This conclusion is also consistent with the results of the calculation of Chang and Temkin (1969). The procedure of Crompton, Gibson, and Robertson (1970) was to assume that the vibrational cross section of, e.g., Burrow and Schulz (1969) was correct, and then to calculate a rotational cross section such that both the calculated rotational cross section and the directly measured vibrational cross section gave agreement between measured and calculated transport data. When they employed this procedure with the vibrational cross sections of either Burrow and Schulz (1969) or Ehrhardt, Langhans, Linder, and Taylor (1968), they found they had to assume unrealistic rotational excita-

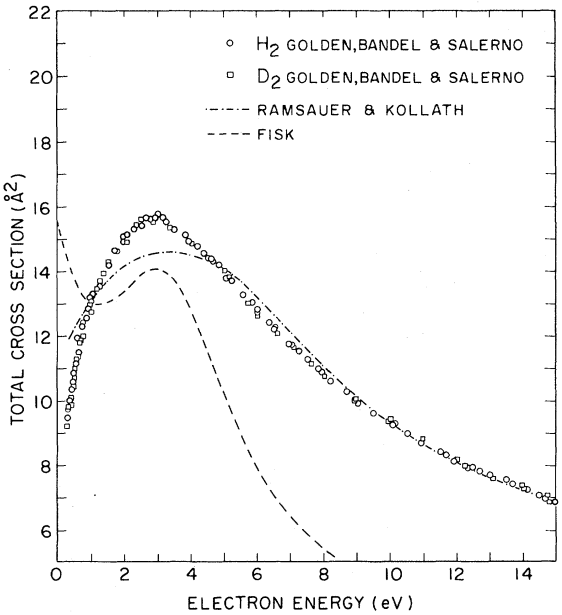

FIG. 16. Total cross sections for e^-–H_2, from Golden, Bandel, and Salerno (1966); Ramsauer and Kollath (1930); and Fisk (1936).

[22] See also Schulz and Asundi (1967).

[23] It should be noted that Burrow and Schulz (1969) also have measured the cross section for vibrational excitation near threshold in H_2 for $v=0\rightarrow2$, 3, 4; in D_2 for $v=0\rightarrow1$, 2; in N_2 for $v=0\rightarrow1$, 2; and in CO for $v=0\rightarrow1$, 2. For vibrational excitation of CO_2 by electron impact, see Boness and Schulz (1968).

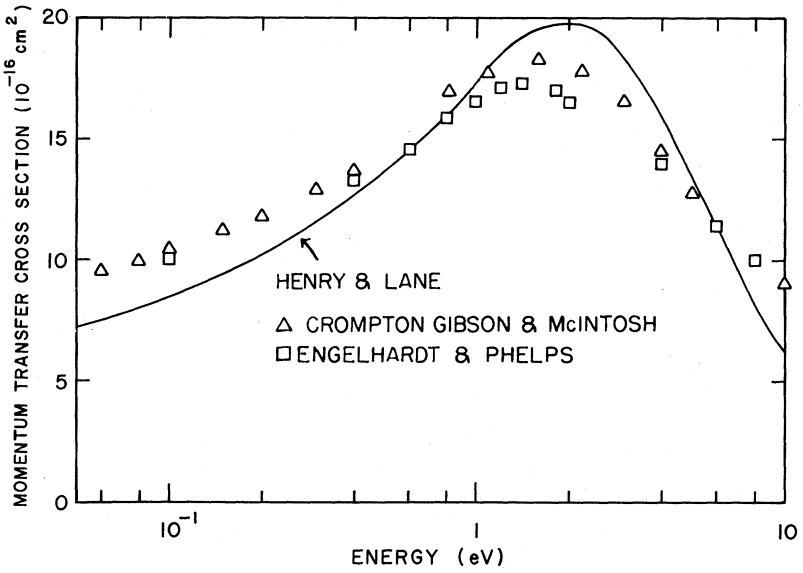

FIG. 17. Momentum-transfer cross sections for e^-–H_2 from Crompton, Gibson, and McIntosh (1969); Engelhardt and Phelps (1967); Henry and Lane (1969).

tion cross sections.[24] In this fashion they infer that the vibrational threshold behavior is that given originally by Crompton, Gibson, and McIntosh (1969). They also estimated an upper limit to the vibrational excitation cross section. Crompton, Gibson, and Robertson's inferred rotational cross sections, along with some of the aforementioned vibrational cross sections near the vibrational threshold, are shown on Fig. 22.

Recently there has been an experiment by Linder (1969) to measure directly the simultaneous rotational–vibrational excitation of H_2. This was a molecular beam experiment, wherein the differential cross section was measured from about 0.3–10 eV using an electrostatic monochromator to make a primary electron beam with 0.02 eV resolution, and then analyzing the scattered electrons as to energy and angle.[25] Figure 23 shows the

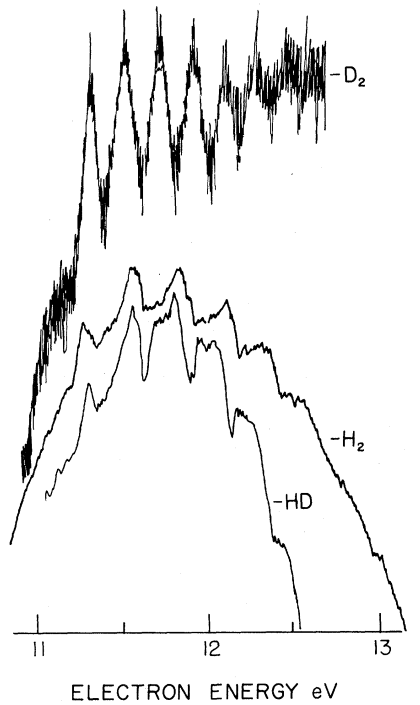

FIG. 18. Transmitted electron current in H_2, D_2, and HD for electrons which have suffered no energy loss as a function of electron energy, at electron energies from abut 11–13 eV (Kuyatt, Simpson, and Mielczarek, 1966).

[24] This conclusion already had been reached by Crompton, Gibson, and McIntosh (1969) with regard to the data for vibrational excitation given by Ehrhardt, Langhans, Linder, and Taylor (1968).

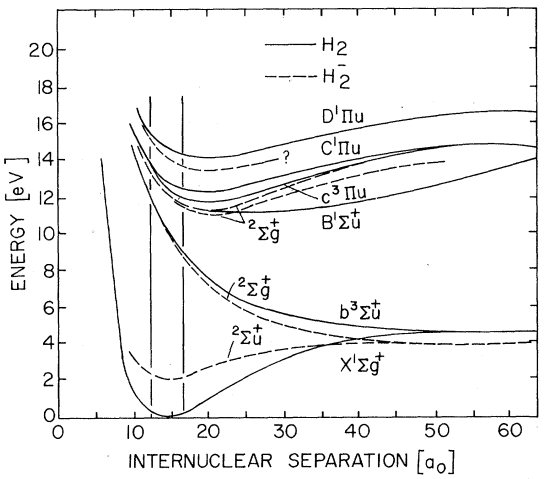

FIG. 19. Some potential energy curves for H_2 and resonant energy states of H_2^-, from Weingartshofer, Ehrhardt, Hermann, and Linder (1970). The area between the two vertical straight lines represents the Franck–Condon region for excitation from the ground vibrational and electronic state of H_2.

[25] For an earlier direct experiment in the same apparatus, giving a measurement of rotational excitation, see Ehrhardt and Linder (1968).

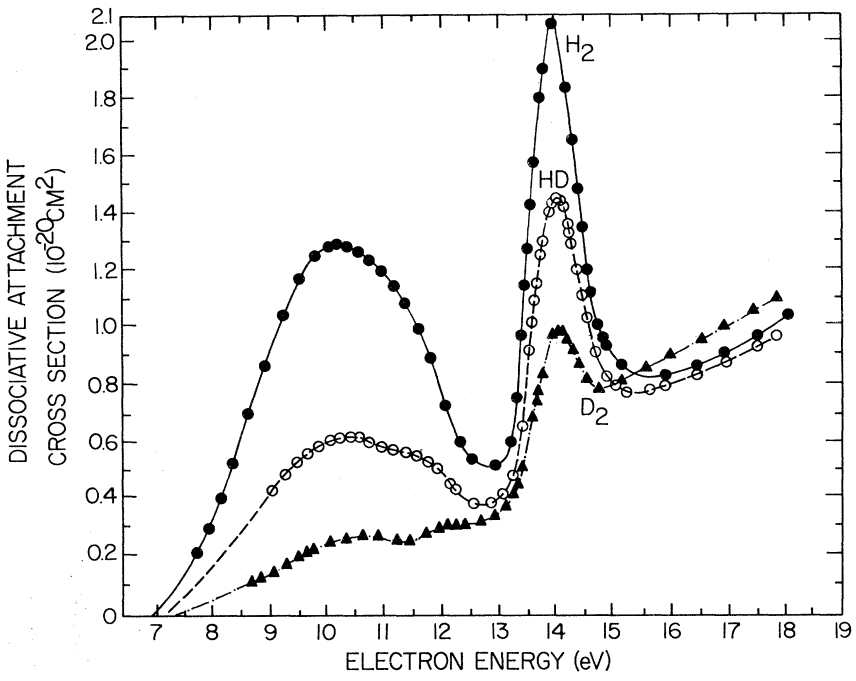

FIG. 20. Cross section for dissociative attachment for electrons on H_2, HD, and D_2, from Rapp, Sharp, and Briglia (1965).

energy loss spectra for e^-–H_2 at three different scattering angles for an incident energy of 4.42 eV. Here we see the pure vibrational excitation as the central large peak. Several rotational transitions may be seen to the left, and superelastic processes may be seen to the right of the central peak. The relative intensities of the rotational transitions are consistent with values calculated from the relative cross section formulas of Gerjuoy and Stein (1955a); for a more careful comparison of Linder's (1969) data with theory, including comparison of the absolute as well as relative intensities, see Sec. 3 below.

Figure 24 shows the integrated cross section [normalized to the total cross section of Golden, Bandel, and Salerno (1966)] for pure vibrational excitation (the upper curve), and the cross section for simultaneous rotational–vibrational excitation (the lower curve). It will be noted that the cross section for simultaneous vibrational-rotational excitation is of the same order as that for pure vibrational excitation; this probably is an important fact which had been ignored previously. With this remark we conclude this chapter, adding only that more e^-–H_2 rotational excitation data will be found in a number of the figures in Secs. 3 and 4 below.

3. CLOSE COUPLING CALCULATIONS OF ELASTIC AND ROTATIONAL EXCITATION CROSS SECTIONS FOR e^-–H_2 COLLISIONS

The preceding section has been devoted to a review of experimental techniques for measuring low-energy electron–molecule collisions, and to a summary of some of the data thus obtained. In this section, we shall examine the ability of close-coupling theory to predict cross sections for elastic scattering and rotational excitation in e^-–H_2 collisions, observations of which were summarized at the end of Sec. 2. But before getting into the details of close coupling theory, which

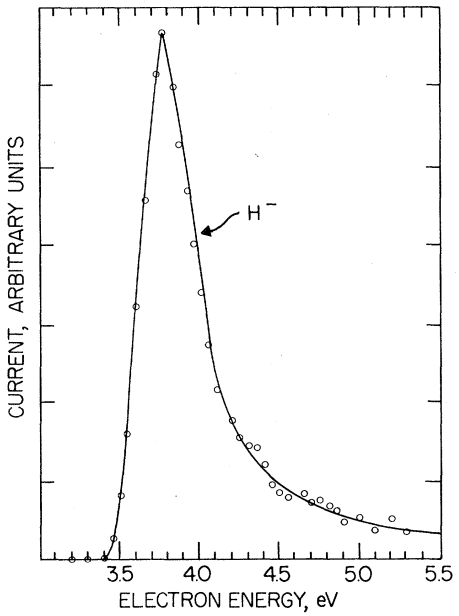

FIG. 21. The H^- ion current from the reaction $e^-+H_2 \rightarrow H^-+H$, as a function of electron energy for energies in the vicinity of 3.73 eV (Schulz and Asundi, 1965).

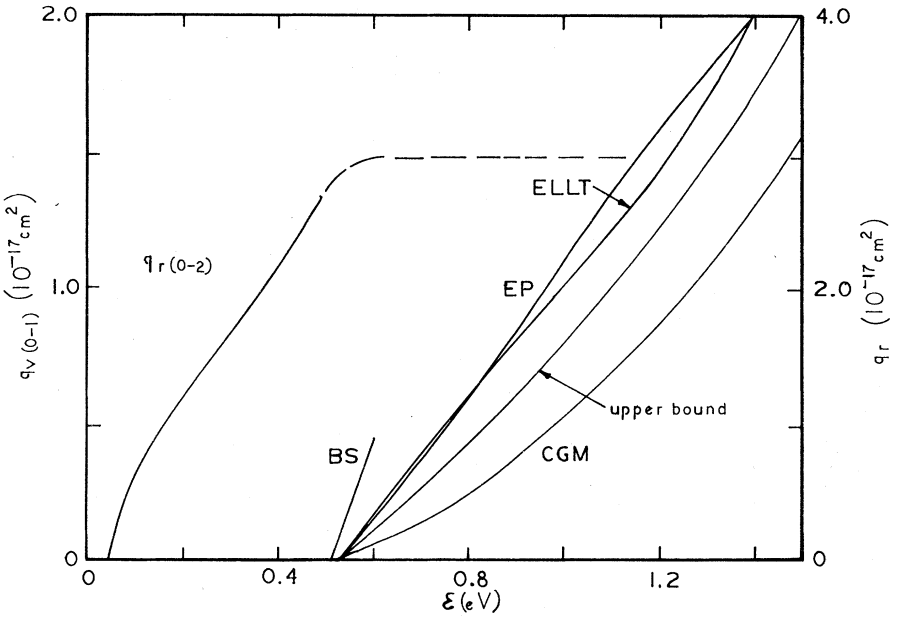

FIG. 22. Cross sections in e^-–H_2 collisions for rotational excitation (q_r) and for vibrational excitation (q_v) in the vicinity of the vibrational excitation threshold, as a function of incident electron energy (Crompton, Gibson, and Robertson, 1970). Their results agree with those of Crompton, Gibson, and McIntosh (1969). Also shown are results of Engelhardt and Phelps (1963), Ehrhardt, Langhans, Linder, and Taylor (1968); Burrow and Schulz (1969); and an estimated upper bound to q_v (Crompton, Gibson, and Robertson, 1970).

can be formal and nontransparent, it is desirable to make a few qualitative remarks.

A primary distinction between electron–atom and electron–molecule collisions is the assuredly anisotropic charge distribution of the target in the latter case. In the case of rotational excitation, this anisotropy is particularly important in that, classically speaking, its interaction with the incident electron provides the necessary torque required to change the angular momentum of the molecule. One then might expect rotational excitation to be favored by a long "lever arm", and it is indeed found that the long-range portion of the electron–molecule anisotropic interaction dominates the rotational-excitation process at low energies. In fact, as has already been mentioned in Sec. 1, for homonuclear diatomic target molecules the pure r^{-3} electron–quadrupole interaction is sufficient to describe rotational excitation, at least in the immediate vicinity of threshold (Gerjuoy and Stein, 1955a). Dalgarno and Moffett (1963) further demonstrated that the r^{-4} adiabatic polarization interaction, also anisotropic, is important just above threshold, and can lead to much larger cross sections at higher energies. However, the question of how to include polarization has remained for some time and, although much progress has been made, is still not completely resolved, at least in the context of close coupling. The inclusion of an explicit polarization potential of this r^{-4} type assumes that the bound molecular electrons relax adiabatically in the field of the scattering electron. Such an assumption is clearly bad at high incident energies, and even the low-energy range of applicability is not certain.

In a sense, the employment of an adiabatic polarization potential is the complement to the fixed-nuclei approximation which was described briefly in Sec. 1, and whose utility in rotational excitation will be the primary subject of Sec. 4. At incident electron energies so low that only rotational excitation channels are open, the incident electron speed has the convenient property of being small compared to electron speeds in the target

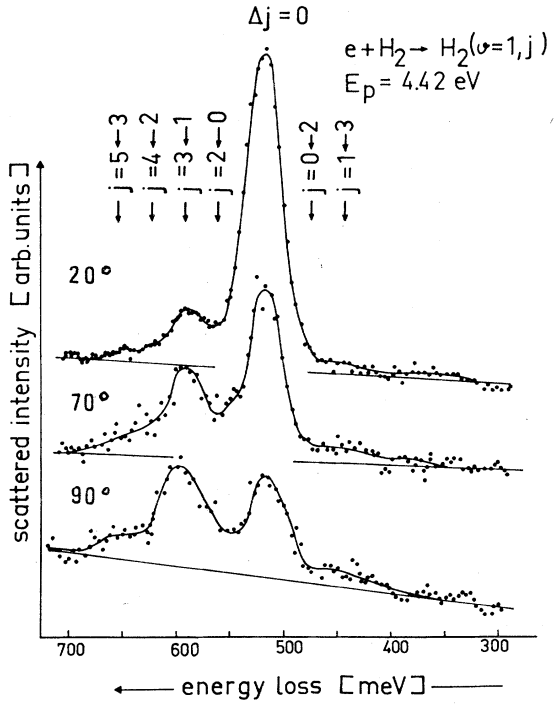

FIG. 23. Energy loss spectra for electrons on hydrogen at three different scattering angles (20°, 70°, and 90°), showing pure vibrational excitation $v=0\rightarrow1$, $\Delta j=0$ as well as simultaneous rotational transitions with $\Delta j=\pm2$, for an incident electron energy of 4.42 eV (Linder, 1969).

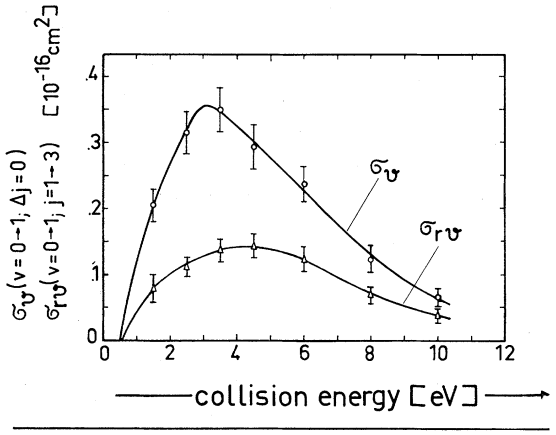

FIG. 24. Total cross sections for pure vibrational (σ_v) and simultaneous rotational–vibrational (σ_{rv}) excitation of H_2 by electron impact (Linder, 1969).

molecule (making plausible the assumption that the target electrons can relax adiabatically in the field of the incident electron), while simultaneously being large compared to the rotational speeds of the target nuclei (making plausible the fixed-nuclei approximation). In this chapter we do not employ the fixed-nuclei approximation, but do make use of—and critically examine—the adiabatic assumption that the target electrons can be supposed to move in the field of an essentially fixed incident electron.

3.1 General Formulation of Rotational Close-Coupling Theory

In this subsection, an attempt will be made to outline the close-coupling theory of electron–molecule scattering in some generality, in order that our descriptions of the calculations actually carried out so far may be meaningful. The complete Schrödinger Equation of the molecule is given by

$$[\mathcal{H}^{(m)}(1,2;\mathbf{R})-E_\alpha^{(m)}]\Psi_\alpha^{(m)}(1,2,\mathbf{R})=0, \quad (3.1)$$

where $\mathbf{R}$ is the internuclear vector, $\mathcal{H}^{(m)}$ is the full molecular Hamiltonian, $\Psi_\alpha^{(m)}$ the full molecular wave function, and $E_\alpha^{(m)}$ the eigenvalues. The index $\alpha=[n, \Lambda, S, M_S, v, j, m_j]$ labels all quantum numbers (among which n includes symmetry character) and, in addition, orders the energies of states, otherwise alike in quantal description; Λ is the projection of electronic angular momentum on the body axis; S and M_S refer to the total spin; v denotes the vibrational state; and j and m_j refer to the rotational angular momentum.

In the Born–Oppenheimer approximation, the total molecular wavefunction may be written [ignoring the Λ degeneracy, as is legitimate for our present purpose]

$$\Psi_\alpha^{(m)}(1,2;\mathbf{R}) = \psi_{n\Lambda S}(1,2;R)\mathfrak{S}_{SM_S}(1,2)\chi_{n\Lambda Sv}(R)\mathfrak{R}_{j\Lambda m_j}(\hat{\mathbf{R}}) \equiv (\psi\mathfrak{S}\chi\mathfrak{R})_\alpha \quad \text{"target states"}, \quad (3.2)$$

where the parts of the function, left to right, are (ψ) spacial electronic, ($\mathfrak{S}$) spin, (χ) vibrational, and ($\mathfrak{R}$) rotational. It will be convenient to think of the full wavefunction as labeled by an index α as shown. An approximate expression for the energy levels is (Herzberg, 1950)

$$E_\alpha^{(m)}\cong E_{n\Lambda S}+a_{n\Lambda S}(v+\tfrac{1}{2})+b_{n\Lambda Sv}\,j(j+1) \quad (3.3)$$

where for the ground $^1\Sigma_g^+$ state of H_2, $a\cong0.54$ eV, and $b\cong0.0075$ eV.

We now consider the electron–molecule system. The process of interest involves the scattering of an electron by H_2 with the possibility of an internal change of state, $\alpha\to\alpha'$. Our task is to obtain positive energy solutions of the full Schrödinger equation

$$(\mathcal{H}_T-E_T)\Psi_T=0,$$
$$\mathcal{H}_T=T_3+V_3(1,2,3;\mathbf{R})+\mathcal{H}^{(m)}(1,2,\mathbf{R}) \quad (3.4)$$

where we may suppose (although of course all electrons are equivalent) that the molecule is initially composed of electrons 1 and 2. In this event, $\mathcal{H}^{(m)}$ is as in Eq. (3.1); T_3 is the kinetic energy of electron 3; and V_3 is the interaction between particle 3 and the initial molecule. The total wavefunction Ψ_T must satisfy scattering boundary conditions, symbolically written

$$\lim_{r_3\to\infty}\Psi_T\sim(\text{plane wave})\Psi_\alpha^{(m)} + \sum_{\alpha'}(\text{scattered waves})_{\alpha'}\Psi_{\alpha'}^{(m)}. \quad (3.5)$$

The amplitudes of the scattered waves then yield cross sections for all possible processes. The total wavefunction must be completely antisymmetric in the space and spin coordinates of all the electrons, and of course can be obtained only approximately.

As has been explained in Sec. 1, the first step in the close-coupling method involves expansion of the total wavefunction in terms of the complete set of target states. In the e^-–H_2 collision of present interest, this expansion of the total wavefunction is given by

$$\Psi_\mu=\mathfrak{A}\sum_{\mu'}r_3^{-1}u_{\mu'\mu}(r_3)(\psi\mathfrak{S}\chi\mathfrak{R})_{\alpha'}Y_{l'm_{l'}}(\hat{\mathbf{r}}_3)\phi_{ml'}(3) \quad (3.6)$$

where $\mu=[\alpha, l, m_l, m_s]$ is an index identifying a particular scattering channel, and $\mathfrak{A}$ denotes the operation of full antisymmetrization. In a typical term, $(\psi\mathfrak{S}\chi\mathfrak{R})_{\alpha'}$ represents the target (H_2) function, treated as if it is exact, $\phi_{ms'}$ denotes the spin function for the continuum electron; and the spherical harmonic carries the angular dependence of $\mathbf{r}_3$, leaving the radial continuum function $u(r_3)$ to be determined. It is well known, however, that the problem is simplified if one takes advantage of the rotational invariance of the full Hamiltonian by first coupling the rotational ($\mathbf{j}$) and orbital ($\mathbf{l}$) angular momenta to form a total angular momentum $\mathbf{J}$, which commutes with $\mathcal{H}_T$ (Arthurs and Dalgarno, 1960). Similarly, it is convenient to couple

the spins to form $\mathbf{S}_T$. This angular momentum coupling is incorporated into the close-coupling method by simply using eigenfunctions of the total angular momenta in place of the product functions. Thus, defining the new functions $\mathcal{Y}$ and $\mathcal{S}$, the expansion of Ψ_T becomes

$$\Psi_\gamma = \mathfrak{A} \sum_{\gamma'} r_3^{-1} u_{\gamma'\gamma}(r_3)\,(\psi\chi\mathcal{Y}\mathcal{S})_{\gamma'}, \tag{3.7}$$

where the "incident" channel index $\gamma=[n, \Lambda, S, v, j, l; J, M, S_T, M_{S_T}]$, and where

$$\begin{aligned}\mathcal{Y}_\gamma &\equiv \mathcal{Y}_{j\Lambda l}^{JM}(\hat{\mathbf{r}}_3, \hat{\mathbf{R}}) \\ &= \sum_{m_j, m_l} (jm_j lm_l \mid JM)\, Y_{lm_l}(\hat{\mathbf{r}}_3)\, \mathcal{R}_{j\Lambda m_j}(\hat{\mathbf{R}}), \\ \mathcal{S}_\gamma &\equiv \mathcal{S}_{S1/2}^{S_T M_{S_T}}(123) \\ &= \sum_{M_S, m_s} (SM_S \tfrac{1}{2} m_s \mid S_T M_{S_T})\, \mathcal{S}_{SM_S}(12)\, \phi_{m_s}(3),\end{aligned} \tag{3.8}$$

the coefficients being the familiar Clebsch–Gordon coefficients. The advantage of using the coupled representation is that the resulting coupled equations turn out to be diagonal in the four quantum numbers J, M, S_T and M_{S_T}, and the radial functions are independent of M and M_{S_T}.

The coupled equations which must be solved to obtain the radial continuum functions are (atomic units are used throughout)

$$\begin{aligned}&\{(d^2/dr_3^2) - [l'(l'+1)/r_3^2] + k_{\gamma'\gamma}^2\} u_{\gamma'\gamma}(r_3) \\ &\qquad - 2\sum_{\gamma''} \langle \gamma' \mid V_3 \mid \gamma'' \rangle u_{\gamma''\gamma}(r_3) \\ &= -2r_3 \sum_{\gamma''} \langle \gamma' \mid \mathcal{H}_T - E_{T_\gamma} \mid (P_{13}+P_{23}) r_3^{-1} u_{\gamma''\gamma}(r_3) \mid \gamma'' \rangle,\end{aligned} \tag{3.9}$$

where γ is designated as the initial system state; $\frac{1}{2}k_{\gamma'\gamma}^2 = (E_{T_\gamma} - E_{\gamma'^{(m)}})$ is the kinetic energy of a scattered electron at ∞, leaving the molecule in state α' (included in γ'); and P_{ij} interchanges electrons i and j. Two kinds of matrix elements influence the scattering. The "static" matrix element on the second line of Eq. (3.9) is simply an integral over all coordinates except r_3 of the electron–molecule electrostatic potential sandwiched between two system state functions. The "static" terms contain all the long-range interactions, and tend to dominate the scattering of high partial waves. These static terms dominate the rotational excitation at low energies. The exchange matrix elements, which appear on the third line of Eq. (3.9), decrease exponentially in r_3, since the operators P_{13} and P_{23} interchange the continuum and bound electrons.

The radial functions must satisfy the asymptotic conditions

$$\begin{aligned}\lim_{r_3\to\infty} u_{\gamma'\gamma} &\sim \delta_{\gamma'\gamma} \exp[-i(k_{\gamma\gamma} r_3 - \tfrac{1}{2} l\pi)] \\ &\quad - (k_{\gamma\gamma}/k_{\gamma'\gamma})^{1/2} S_{\gamma'\gamma} \exp[i(k_{\gamma'\gamma} r_3 - \tfrac{1}{2} l'\pi)] \qquad k_{\gamma'\gamma}^2 > 0 \\ &\sim \exp(-\mid k_{\gamma'\gamma} \mid r_3) \qquad k_{\gamma'\gamma}^2 < 0\end{aligned} \tag{3.10}$$

which define the "scattering matrix" $\mathbf{S}$. For channels not energetically accessible, i.e., "closed channels", the radial functions are seen to decay exponentially.

Knowledge of the $\mathbf{S}$ matrix allows calculation of the differential and integrated cross section for molecular excitation. The cross section, averaged over initial, and summed over final magnetic quantum numbers, is given by

$$\begin{aligned}&\sigma(n'\Lambda'S'v'j' \leftarrow n\Lambda Svj) \\ &\quad = \pi[k_{\gamma\gamma}^2 (2j+1)(2S+1)(2s+1)]^{-1} \\ &\quad \times \sum_{JS_T ll'} (2J+1)(2S_T+1) \mid \delta_{\gamma'\gamma} - S_{\gamma'\gamma} \mid^2,\end{aligned} \tag{3.11}$$

where, of course, $s=\frac{1}{2}$.

3.2 Elastic Scattering and Rotational Excitation of H_2

The close-coupling approximation is obtained by making some hopefully wise truncation of the set of coupled Eqs. (3.9). The first attempt at a close coupling calculation for electron–molecule scattering was made by Lane and Geltman (1967). Since only the ground electronic state $X\,^1\Sigma_g^+$ was included, the effects of polarization, which can be described in terms of virtual electronic excitation (Castillejo, Percival, and Seaton, 1960), were not being taken into account. The internuclear separation was taken as fixed at the equilibrium value, $R_e = 1.4a_0$, and the exchange matrix elements were ignored. It was expected that this latter approximation would primarily affect the s-wave scattering, felt at that time to be unimportant in rotational excitation. The electron–molecule polarization, however, being a long-range and anisotropic interaction, was known to be important (Dalgarno and Moffett, 1963) and was included in a phenomenological manner. For purposes primarily of illustration, a short-range modification of the potentials was made to "mock" the effects of exchange.

The matrix elements which appear in the coupled equations for the radial scattering function can be reduced to angular integrals (we will drop the subscript on $\mathbf{r}_3$ from here on, writing $\mathbf{r}$),

$$\langle \gamma' \mid V \mid \gamma'' \rangle = \langle j'l'JM \mid V(\mathbf{r}, \hat{\mathbf{R}}) \mid j''l''JM \rangle, \tag{3.12}$$

where $V(\mathbf{r}, \hat{\mathbf{R}})$ can be considered an effective e^-–H_2 interaction potential. It is in fact just the electrostatic electron–H_2 potential, averaged over the electronic ground state of the molecule and evaluated at the equilibrium separation $R_e = 1.4a_0$. The homonuclear nature of H_2 permits an expansion in even harmonics of $\cos\theta$ of the form

$$V(\mathbf{r}, \hat{\mathbf{R}}) = V_0^W(r) + V_2^W(r) P_2(\cos\theta) + \cdots, \tag{3.13}$$

where θ is the angle between $\mathbf{r}$ and $\hat{\mathbf{R}}$. The superscript W is just a reminder that the Wang $X\,^1\Sigma_g^+$ function was used here (Wang, 1928). The spherical term $V_0^W(r)$ will not contribute to rotational excitation, and the leading anisotropic term imposes a selection rule[26] on rotational excitation of $\Delta j = \pm 2$.

[26] This selection rule is discussed in Sec. 4 below.

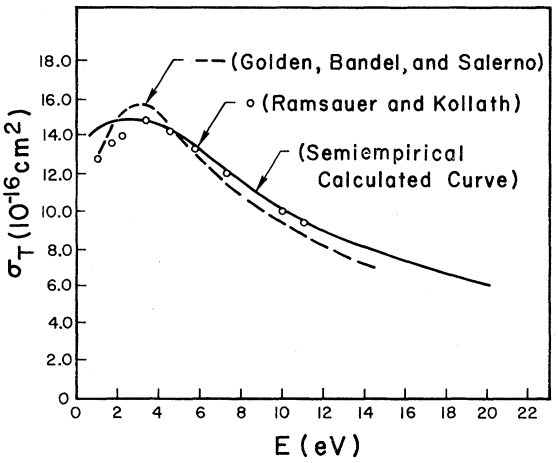

FIG. 25. Total cross sections σ_T for e^-–H_2 scattering. Dashed curve, experimental results of Golden, Bandel, and Salerno (1966); open circles, Ramsauer and Kollath (1930); solid curve, the semiempirical calculations of Lane and Geltman (1967).

These potentials were modified by adding long-range terms, which include the electron–molecule polarization and insure that the electron–molecule interaction is correct at large r. These modifications are necessary because the manner in which the Wang molecular wave function was used results in exponentially decreasing V_0^W and V_2^W at large r, which cannot be correct, if only because the molecule is known to possess a nonvanishing quadrupole moment. The modified functions were of the form

$$V_0(r)=V_0^W(r)B(r)-(\alpha/2r^4)C(r),$$
$$V_2(r)=V_2^W(r)B(r)-(\alpha'/2r^4+Q/r^3)C(r), \quad (3.14)$$

where the values $\alpha=5.50a_0^3$, $\alpha'=1.38a_0^3$, and a quadrupole moment $Q=0.49ea_0^2$ were used. The long-range terms were cut off with the function

$$C(r)=1-\exp[-(r/R_c)^6],$$

where R_c was determined from observed elastic scattering data, as discussed below. This is really the only parameter which affects the rotational excitation cross section. The short-range attractive terms were multiplied by the function

$$B(r)=\exp[-B(R_e/2-r)], \quad r\leq R_e/2$$
$$=1, \quad r>R_e/2, \quad (3.15)$$

which contains a strength parameter B. Note that the somewhat arbitrary $B(r)$ is effective only well inside the molecule; the effect of $B(r)$ is to make the short-range field more attractive. This short-range modification was found to have no effect on the rotational excitation cross sections.

Using the potentials just described, elastic ($j=0$) and rotational excitation ($j=0\rightarrow2$) cross sections were calculated for several values of the long-range parameter R_c, and short-range parameter B. It was found that p wave and higher partial-wave scatterings were insensitive to a moderate variation of the short-range potential via the parameter B. Thus, B was chosen to be $-3a_0^{-1}$, in order to obtain reasonable s-wave elastic scattering at low energies where it dominates the total scattering cross section.

The long-range cutoff parameter R_c was found to influence both s- and p-wave scattering. However, above about 5 eV, only p-wave and higher partial-wave scattering showed sensitivity to R_c. Since s and p waves dominate the elastic cross section in this energy range, it was felt that choosing the cutoff parameter R_c so as to yield reasonable elastic scattering for energies $E\gtrsim5$ eV, would result in a reasonable representation of p-wave scattering and hence of the rotational excitation. Values of R_c in the range $1.8a_0$–$2.0a_0$ were found to be satisfactory.

In Fig. 25 we have replotted as a smooth curve (dashed) the total cross section points from Fig. 16, measured by Golden, Bandel, and Salerno (1966). Figure 25 also shows (open circles) the total cross sections measured by Ramsauer and Kollath (1930), which in Fig. 16 were represented by the smoothed dot–dash curve. The solid curve in Fig. 25 shows the calculated total cross section (elastic plus rotational excitation), computed as described above with the cutoff parameter $R_c=1.8a_0$. The agreement is seen to be very good. Because this theory (Lane and Geltman, 1967) contains adjustable parameters, and therefore is not ab initio in the sense explained in Sec. 1, the calculated curve has been labeled "semi-empirical" in Fig. 25. However, the present calculation must be distinguished from the older much less sophisticated and less successful semiempirical calculations of Fisk (dashed curve in Fig. 16), which will be discussed in Sec. 4. Coincidentally, the theoretical curve in Fig. 25 is in better agreement with the Ramsauer measurements. A slightly larger value of R_c would make agreement with Golden, Bandel, and Salerno (1966) better. A precise fit was not important at this juncture.

The cross sections computed by Lane and Geltman (1967) for several individual rotational transitions are given in Fig. 26. It was found that the sum of elastic and excitation cross sections from a given initial rotational level j was quite accurately independent of j. It was conjectured that this was because the rotational periods were large compared to the collision time. Indeed, it will be seen in Sec. 4 that this result is just a reflection of the validity of the adiabatic-nuclei approximation.

A comparison between close-coupling, distorted wave, and Born approximation $j=0\rightarrow2$ rotational excitation cross sections is given in Fig. 27. By Born approximation in this figure is meant a first-order calculation using the full interactions (3.13)–(3.15), to be distinguished from the Gerjuoy–Stein (1955) Born approximation calculation which employed only the pure quadrupole contribution to $V_2^W(r)$, namely $V_2^W=-Q/r^3$ at all r. The distorted wave curve in Fig. 27

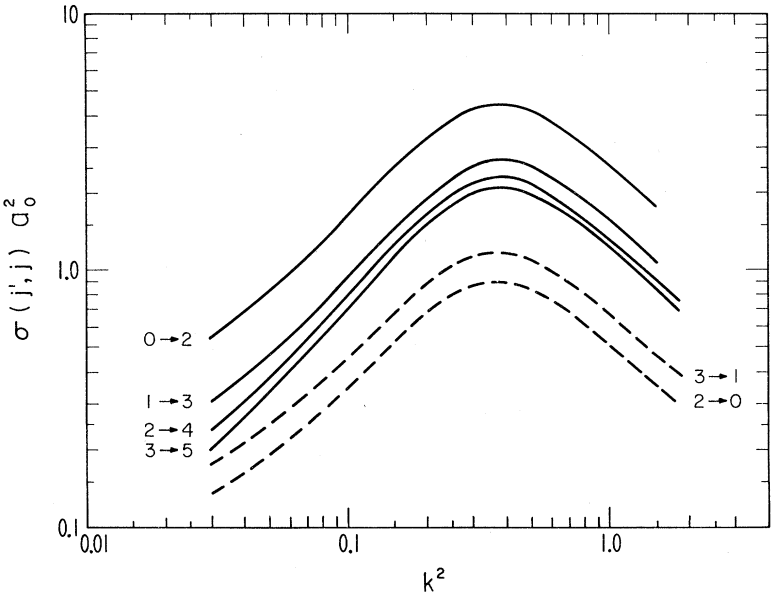

FIG. 26. Calculated e^-–H_2 rotational excitation cross sections, from Lane and Geltman (1967). The energy scale is in atomic units, with $k^2=1$ at an energy of one Rydberg.

lies very near the close-coupling curve, indicating that solutions to the close-coupling equations are reasonably approximated by neglecting coupling between the channels in first order (reflecting the fact that the rotational coupling is comparatively weak in e^-–H_2 collisions); on the other hand, the Born curve in Fig. 27 lies well below the close-coupling and distorted-wave curves away from threshold, indicating that the further approximation of neglecting distortion in the scattering electron wave function is poor.

In Fig. 28, these Lane and Geltman (1967) close-coupling results for two values of the long-range cutoff parameter, $R_c=1.8$ and $2.0a_0$ (labeled *LG* in Fig. 28) are compared with earlier calculations, namely Geltman and Takayanagi (1966); Sampson and Mjolsness (1965); Dalgarno and Moffett (1963); Oksyuk (1966); Dalgarno and Henry (1965); and Gerjuoy and Stein (1955a). It is evident that near threshold (excepting Oksyuk, who fails to include long range interactions) all the more complicated calculations converge to the simple Gerjuoy–Stein pure quadrupole interaction Born approximation formula. The recent results of Chang and Temkin (1969) and Hara (1969b) are not included in Fig. 28, but will be discussed in Sec. 4.

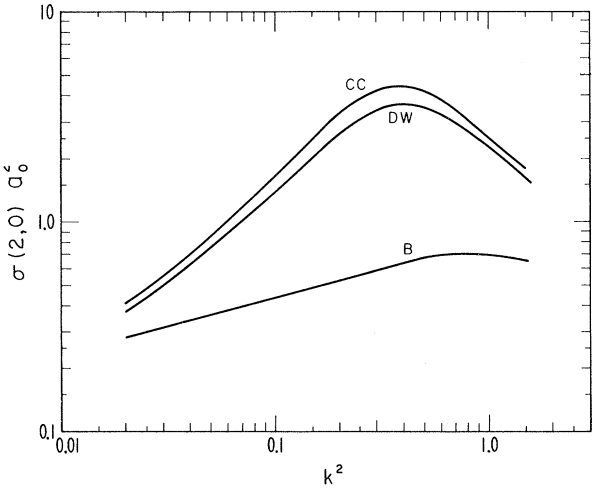

FIG. 27. Comparison of calculated $j=0\rightarrow2$ rotational excitation cross sections obtained in the close-coupling (CC), distorted-wave (DW), and Born approximation (B) using the full interactions (3.13)–(3.15), from Lane and Geltman (1967).

In order to better judge these first close-coupling calculations, it might be helpful to look ahead a bit and compare in Fig. 29 the calculated $j=1\rightarrow3$ cross sections with the measurements Ehrhardt and Linder (1968) made a few years later.[27] The solid curve represents the calculation, and the dashed curve through open circles, the measurements. Error bars of about 10% to 15% should appear on experimental points. The open triangles are their slightly earlier measurements. At the energies below the peak in Fig. 29, where p waves make the main contribution to the rotational excitation cross section (see Sec. 4 below), Fig. 29 suggests that the tail of the long-range potential used in this early calculation (Lane and Geltman, 1967) is still too weak.

In order to further illustrate the nature of these early results, we compare in Fig. 30 differential $j=1$ elastic

[27] We acknowledge with thanks private communications from Ehrhardt and Linder on the subject of their measurements. *Note added in proof*: The $j=1\rightarrow3$ experimental points in Fig. 30 are taken from somewhat different measurements than those in Fig. 43. As a matter of fact, the most recent data (unpublished) on the $j=1\rightarrow3$ angular distribution agree very well with the Chang–Temkin–Hara theoretical predictions shown in Fig. 43. Moreover, the latest data indicate that the Linder (1969) curve in Fig. 34 should be lowered about 10% at energies between 4–6 eV, and raised somewhat at the lower energies, which now make the comparison between experiment and theory for $j=1\rightarrow3$ about as good as in Fig. 33 for $j=0\rightarrow2$.

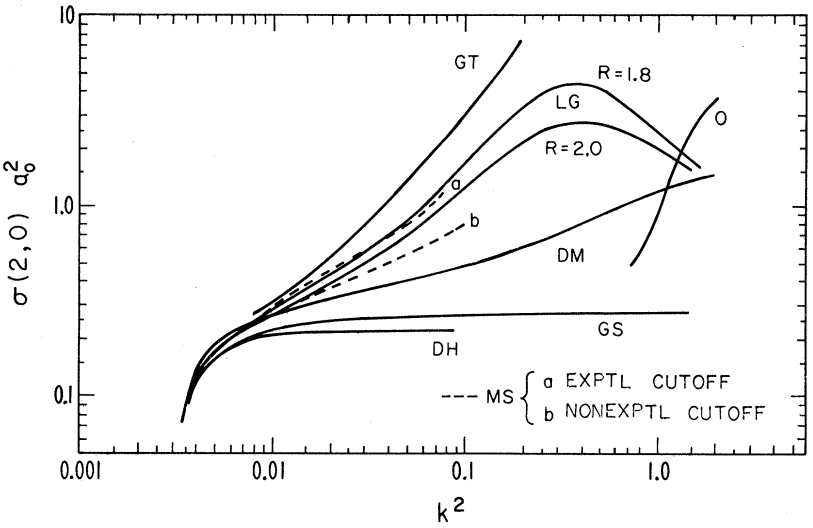

FIG. 28. Calculated $j=0\rightarrow2$ rotational-excitation cross sections: GT, Geltman and Takayanagi (1966); LG, Lane and Geltman (1967); MS, Sampson and Mjolsness (1965), with two different small r cutoffs of the asymptotic potentials; DM, Dalgarno and Moffett (1963); GS Gerjuoy and Stein (1955a); DH, Dalgarno and Henry (1965); O, Oksyuk (1966).

and $j=1\rightarrow3$ rotational excitation cross sections at 4.35 eV. The lower curve and ordinate on the right refer to the elastic cross section; the upper curve and ordinate on the left refer to the inelastic cross section. The circles are the measurements of Ehrhardt and Linder (1968)[27]; the open triangles, Ramsauer and Kollath (1930); and the solid curves the calculated results (Lane and Geltman, 1969). The results of Ehrhardt and Linder are normalized to theory at 90°; however the Ramsauer and Kollath data are absolute. While agreement is satisfactory for the elastic cross section, one cannot say much about the rotational excitation. There seems to be an upward trend in the data at low angles, which is present in the calculated cross sections. The error bars are fairly large due to the difficulty of the measurement. Calculations have been made at other energies and the comparisons are much the same. In Fig. 31 is shown a similar (to Fig. 30) comparison at $E=10$ eV.

There were two particularly disturbing features of these early close-coupling calculations by Lane and Geltman (1967): (1) the need for a semiempirical determination of the polarization interaction, and (2) the neglect of exchange. The polarization question seemed more pressing at the time, so an attempt was made by Lane and Henry (1968) to calculate a reasonable polarization potential from first principles.

The procedure, akin to the well-known polarized orbital method of Temkin (1957), is based on the Rayleigh–Ritz variational principle. A strictly adiabatic approach was taken where the scattered electron 3 was taken to be fixed in space. Employing the variational method, a trial wavefunction of the form

$$\psi(12;3)=\phi_0(12)\sum_{\alpha,\beta\geq0}C_{\alpha\beta}(x_1+x_2)^\alpha(z_1+z_2)^\beta$$

was used to represent the molecule in the field of the electron, where $\phi_0(12)$ was taken to be the one-center Joy and Parr ground-state wavefunction for H_2, here supposed composed of electrons 1 and 2. The linear variational coefficients $C_{\alpha\beta}$ depend of course on the coordinates of electron 3. The secular equation was solved and the minimum eigenvalue, also a function of the coordinates of electron 3, was compared to the unperturbed energy plus the first-order static interaction, the difference being the polarization potential.

The homonuclear symmetry permits an expansion of the polarization potential in terms of even Legendre polynomials of $\cos\theta=\hat{\mathbf{r}}_3\cdot\hat{\mathbf{R}}$. Once the potential has been obtained, it is convenient to drop the subscript 3. The radial coefficients in this polarization–potential expansion are compared in Fig. 32 with the semiempirical potentials of Lane and Geltman (1967) (actually the negative of the potential is plotted). The spherical (subscripted 0) and anisotropic (subscripted 2) functions are plotted separately. There is an apparent qualitative agreement; however, the variational results are smaller for large values of r, where the polarization

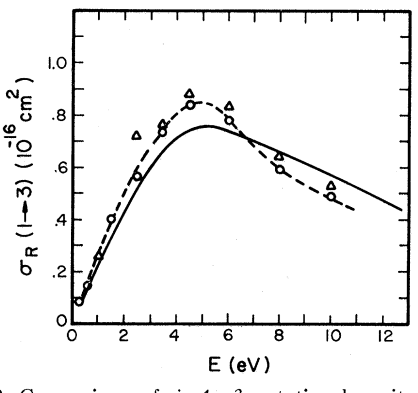

FIG. 29. Comparison of $j=1\rightarrow3$ rotational excitation cross sections: triangles, circles and dashed line, the measurements of Ehrhardt and Linder (1968); solid line, the semiempirical calculation of Lane and Geltman (1967).

interaction is important to the cross section (at smaller values of $r \lesssim 2a_0$, the static potentials $V_0{}^W(r)$ and $V_2{}^W(r)$ are much larger and dominate the scattering). The semiempirical potentials were felt to be larger in magnitude because of their tendency to include p-wave exchange effects which might be present. This comparison suggested that exchange was probably also important for p waves. The two-center polarization potentials calculated by Adamov, Objedkov, and Evarestov (1963), and more recently by Hara (1969a) are somewhat smaller, but generally in good agreement for values of r important to the rotational excitation cross section, i.e., for p-wave scattering.

Using the variationally determined polarization interaction just described, Henry and Lane (1969) began another close-coupling calculation similar to the earlier calculation, but including the exchange matrix elements explicitly in the coupled equations. No adjustable parameters were present. Ardill and Davison (1968) already had reported a distorted-wave calculation of p-wave scattering including exchange, and found the contribution to be significant; they did not, however, include the important polarization effects.

Before the improved close-coupling calculations were completed, Crompton, Gibson, and McIntosh (1969) had begun to obtain $j=0\rightarrow2$ rotational excitation cross sections via electron drift and diffusion measurements in parahydrogen; that parahydrogen observations would provide a good test of the theory had been suggested by Gerjuoy and Stein (1955b). These observations of Crompton, Gibson, and McIntosh (1969) indicate that the early results of Lane and Geltman (1967) were somewhat too small. This observation was consistent with Ehrhardt and Linder's (1968) beam measurements of the $j=1\rightarrow3$ cross section and, in the light of Ardill and Davison's (1968) calculation, seemed to demonstrate conclusively the presence of exchange effects.

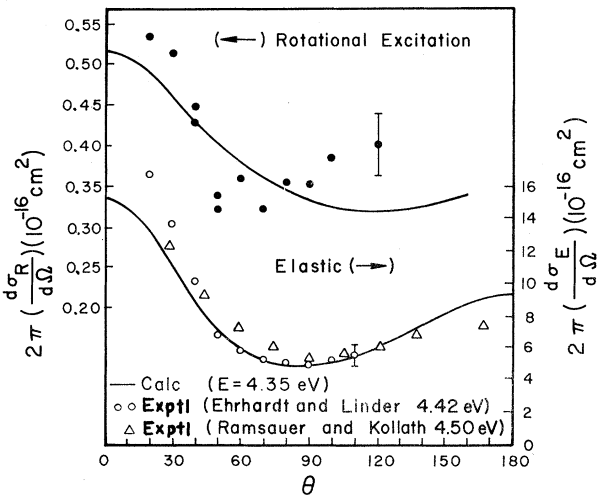

FIG. 30. Differential elastic and $j=1\rightarrow3$ rotational excitation cross sections for energies around $E=4.35$ eV. The calculations are by Lane and Geltman (1969). Open circles and triangles, elastic scattering in the $j=1$ state; closed circles, rotational excitation. See Footnote 27.

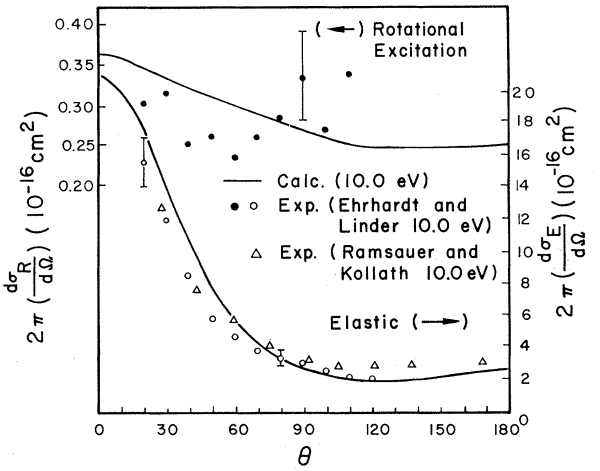

FIG. 31. Differential elastic and $j=1\rightarrow3$ rotational excitation cross sections for $E=10$ eV. The calculations are by Lane and Geltman (1969). Open circles and triangles, elastic scattering in the $j=1$ state; closed circles, rotational excitation. See Footnote 27.

As soon as the new close-coupling results, including exchange, were obtained, they were included in the analysis of swarm data. The results for the $j=0\rightarrow2$ cross section are shown in Fig. 33. The solid curve labeled LG represents the original semiempirical close-coupling results of Lane and Geltman (1967, 1969). The curve labeled A represents the new theoretical results including exchange and polarization (Henry and Lane, 1969). The open squares are swarm data of Crompton, Gibson, and McIntosh (1969). The agreement between these swarm data and curve A is very satisfactory, namely within 2% throughout the energy range from threshold to 0.5 eV. The open circles represent the early swarm measurements of Englehardt and Phelps (1963). The curves B and C also were quoted by Henry and Lane (1969); they include polarization but no exchange (B), and exchange but no polarization (C). Thus both effects are important.

At higher energies, where $j=1\rightarrow3$ transitions are sizable, the agreement between these close-coupling calculations and the measurements is not quite so good—as shown in Fig. 34. The open squares and circles are the $j=1\rightarrow3$ rotational excitation measurements of Ehrhardt and Linder (1968), the squares being the original measurements and the circles more recent results[27]; the open triangles correspond to data reported more recently by Linder (1969). The reason for the significant disagreement between these two sets of data is unclear, but neither of these sets[27] has the kind of overlap with the theoretical calculations of Henry and Lane (1969) seen in Fig. 33.

A number of other theoretical calculations also are shown in Fig. 34. In particular, we see that the original close-coupling semiempirical results of Lane and Geltman (1967, 1969) are somewhat too small as was

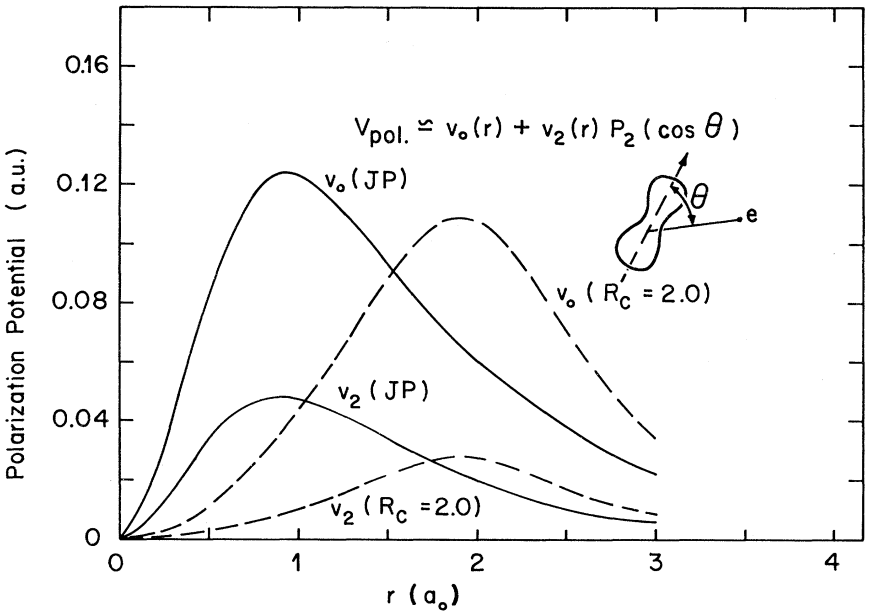

FIG. 32. Polarization potentials: solid curves, Lane and Henry (1968), using the Joy and Parr (JP) ground-state wave function for H_2; dashed curves, Lane and Geltman (1967).

pointed out earlier. The refined close-coupling calculations of Henry and Lane (1969) including exchange and polarization yield cross sections which (if the data can be trusted) appear to be somewhat too large at energies up to 2 eV. A similar observation can be made in the case of $j=0\rightarrow 2$ cross sections (Fig. 33), suggesting that perhaps the magnitude of Henry and Lane's (1969) polarization potential is somewhat too large.

Henry (private communication) has repeated the close-coupling calculations, including the $v=0$ vibrational wavefunction explicitly, rather than assuming the internuclear separation to be fixed at the equilibrium separation. In so doing, however, he has had to make certain assumptions about the dependence of the polarization potentials on the internuclear separation. His results also are shown in Fig. 34. The two lower curves in Fig. 34 again emphasize the need for both polarization and exchange.

With exchange as well as polarization included in the close-coupling calculation we also should expect to be able to represent the s-wave scattering, which is particularly sensitive to short-range effects and which dominates the elastic (and hence total) cross section below a few eV. In Fig. 35, a comparison is given between the calculated (Henry and Lane, 1969) total (elastic plus rotational) cross sections in the states $j=0$ (solid curve A) and $j=1$ (dashed curve A), the measurements of Golden, Bandel, and Salerno (1966), and the measurements of Ramsauer and Kollath (1930). As in Fig. 33, the curve B corresponds to the neglect of exchange but with the polarization included, while curve C corresponds to the neglect of polarization but with exchange included (Henry and Lane, 1969). Thus, we must conclude that both effects are important for elastic scattering as well as rotational excitation. In the vicinity of the maximum the theoretical cross sections computed including both polarization and exchange are somewhat too large. Again this probably reflects too strong a polarization potential.

In Fig. 36 a comparison of several fairly recent elastic scattering calculations is given. The experimental points are the same as described in Fig. 35, and the Henry and Lane (1969) exchange plus polarization close-coupling results are repeated on this figure as a dot–dashed curve. No attempt will be made to discuss each calculation, except to remark that they all include

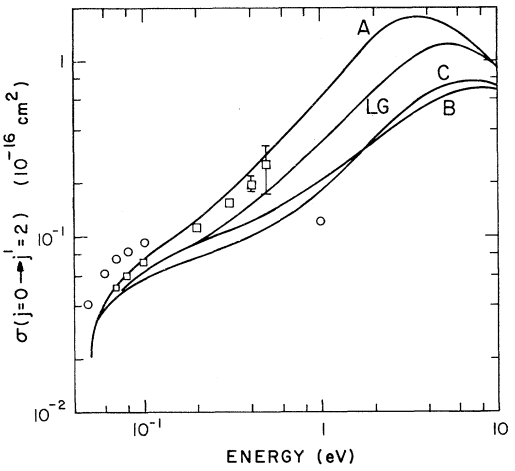

FIG. 33. Comparison of $j=0\rightarrow 2$ rotational excitation cross sections. From Henry and Lane (1969): A, exchange and polarization; B, no exchange; C, no polarization. The curve labeled LG represents the semiempirical calculations of Lane and Geltman (1967, 1969). Open circles, Engelhardt and Phelps (1963); open squares, Crompton, Gibson, and McIntosh (1969).

exchange effects in one form or another, Massey and Ridley (1956) being the first of such calculations (Massey and Ridley's procedures are described in Sec. 4.) We also comment briefly here on the results of Hara's (1969a) recent two-center elastic scattering calculation with and without polarization, although Hara's work is discussed rather fully in Sec. 4 below. Hara's (1969b) polarization potential is somewhat weaker than that of Henry and Lane (1969), which may account for the better agreement he obtains with experiment. The fact that his results neglecting polarization are in such close agreement with the close-coupling treatment, also neglecting polarization (see Fig. 36) is further discussed in the next chapter.

The contents of this chapter, especially comparisons such as those in Figs. 33, 35, and 36, show that we are well on the way toward developing—via the rotational close-coupling approximation—reliable procedures for *ab initio* prediction of elastic and rotational excitation cross sections in slow electron collisions with H_2. For heavier diatomic molecules, the close-coupling equations will be more complicated, and the utility of the approximation still is in question. Even for H_2, in order to further improve the calculations, a full polarized orbital calculation probably will be necessary. Needless to say, processes involving pure vibrational excitation, or simultaneous vibrational and rotational excitation, are more complicated than those we have been discussing, and remain a challenge to the theorist; the possible importance of simultaneous rotational–vibrational excitation was noted at the end of Sec. 2. In fact, accurate inclusion of the vibrational degrees of freedom probably would make the most pertinent improvement in our present theories of electron–molecule scattering. Similarly, the electronic excitation cross sections, with their observed resonance structure (e.g., the observations mentioned in connection with Fig. 18), are a challenge to the close-coupling method, and a substantial effort is being made in this direction at the present time. Many of the other e^-–H_2 observations summarized in Sec. 2 (e.g., dissociative attachment, Sec. 2.33b), offer even more subtle and abstruse challenges to theory, and—though possibly understandable in some respects on the basis of well-founded (not semiempirical) theory, cf. Sec. 4 below—must be considered essentially out of reach of any presently envisaged *ab initio* calculations. For a review of the present status of the theory of dissociative attachment, along with a thorough discussion of the problem of resonant scattering of electrons by molecules, see Bardsley and Mandl (1968). The theory of dissociative recombination, a process resulting from the collision of an electron with a positively charged molecular ion, has been reviewed by Bardsley and Biondi (1970).

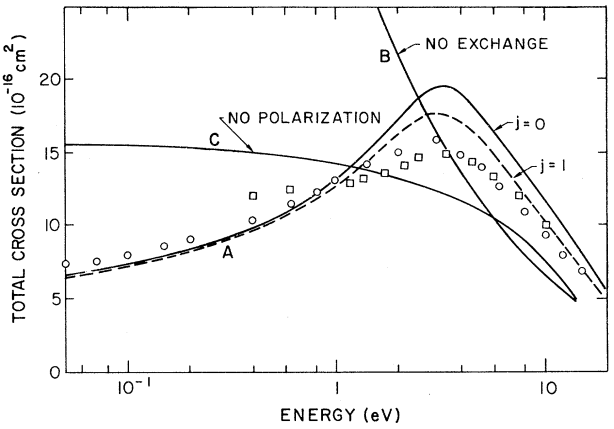

FIG. 35. Comparison of total e^-–H_2 cross sections. Theoretical curves from Henry and Lane (1969): curves A, exchange and polarization (—, $j=0$, and - - -, $j=1$); B, no exchange; C, no polarization. Circles, measurements of Golden, Bandel, and Salerno (1966); squares, measurements of Ramsauer and Kollath (1930).

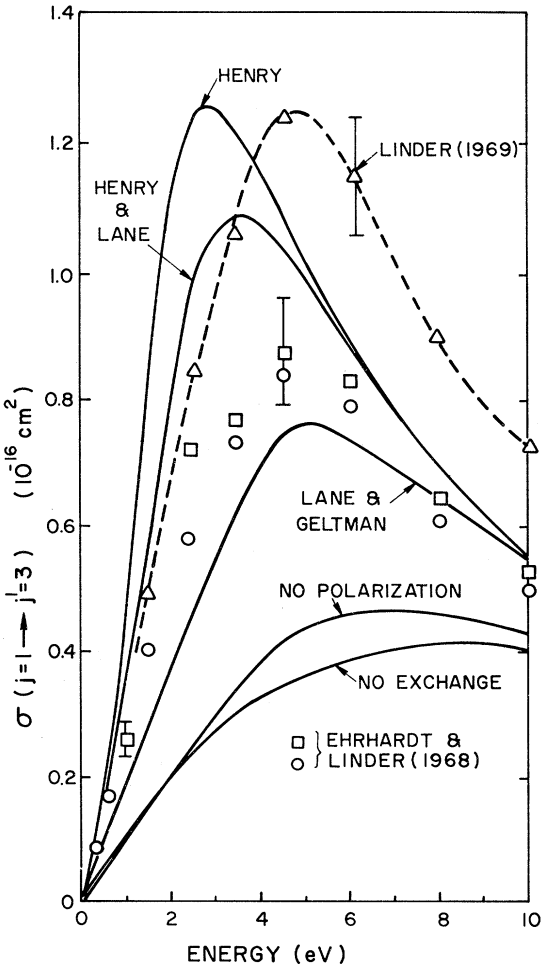

FIG. 34. Comparison of $j=1\rightarrow3$ rotational excitation cross sections. Shown are calculations by: Henry (private communication); Henry and Lane (1969); Lane and Geltman (1967). The no exchange and no polarization curves, computed by Henry and Lane (1969), correspond respectively to curves B and C of Fig. 33. Circles and squares, Ehrhardt and Linder (1968); triangles, Linder (1969). See Footnote 27.

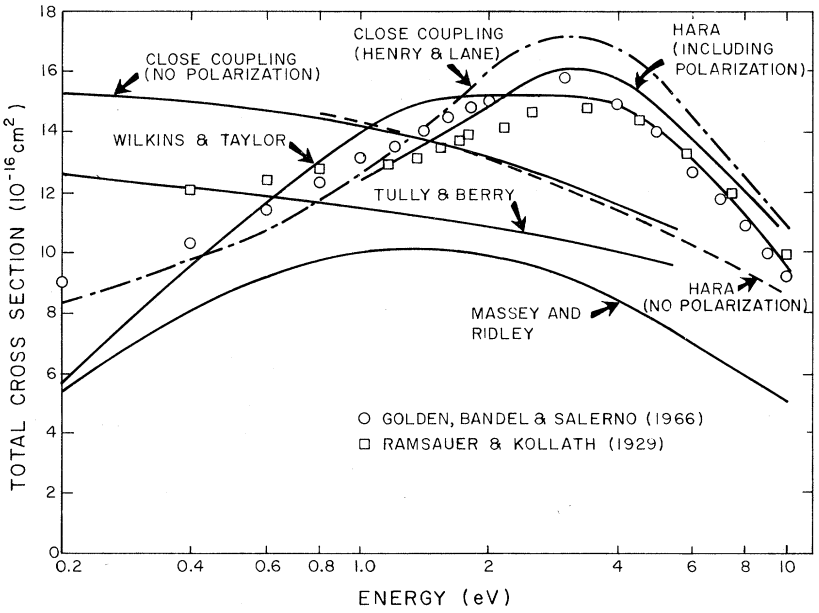

FIG. 36. Comparison of total e^-–H_2 cross sections. All theoretical curves include exchange in one form or another. Theoretical calculations plotted: Henry and Lane (1969) close coupling, with polarization (dot–dash), and without (solid); Hara (1969a) two-center, with polarization (solid), and without (dash); Wilkins and Taylor (1967) but see Footnote 29 below; Massey and Ridley (1956); Tully and Berry (1969). Experimental points from Fig. 35.

4. DEVELOPMENT OF FIXED-NUCLEI APPROXIMATIONS OF ELECTRON–MOLECULE SCATTERING AND THE THEORY OF ROTATIONAL EXCITATION

The previous section has reviewed theoretical computations of e^-–H_2 scattering, calculated from a formalism (Arthurs and Dalgarno, 1960) which, particularly when electron exchange is included (Ardill and Davidson, 1968; Henry and Lane, 1969), naturally fits the description "rotational close coupling". As has been seen (Figs. 33, 35, and 36), rotational close-coupling calculations—especially when polarization is taken into account along with exchange—are capable of very satisfactory agreement with experiment. However, inclusion of exchange and polarization in the rotational close-coupling calculations undeniably is very arduous, even for the simplest molecular target (H_2) at electron energies so low that only a few rotational channels are open.

The intent of this chapter is to examine a technique for computing rotational excitation cross sections which (apparently) can be made less arduous, but no less successful, than the rotational close-coupling procedures. As has been explained in Sec. 1, the reduction in arduousness is attained by starting from a somewhat less fundamental point of view than does close coupling; however, within their frameworks the fixed-nuclei and adiabatic-nuclei approximations we shall describe can be carried out consistently, are physically understandable, and are capable of considerable accuracy. Our examination of the approximations is restricted to electron collisions with homonuclear diatomic molecules; in fact, except for a very brief discussion of e^-–N_2 collisions, this Section like Sec. 3 treats only collisions involving H_2^+ and H_2. In Sec. 4.1 immediately below, we examine the fixed-nuclei approximation yielding elastic scattering amplitudes. In Sec. 4.2, we discuss the use of these fixed-nuclei elastic amplitudes in an adiabatic-nuclei approximation for rotational excitation amplitudes.

4.1 Fixed-Nuclei Theories

The basic idea of this section's approach is supremely simple, and for that reason not new. Specifically, we assume that for the purposes of calculating purely elastic scattering amplitudes the molecule can be replaced by one in which the nuclei are fixed during the whole scattering process. If the electron velocity v is much faster than the nuclear rotational velocities V, this assumption is reasonable (though not rigorous—recall the remarks in Sec. 1 concerning the collision time). In terms of the incident electron energy E, the condition $v>V$ implies $E=\frac{1}{2}mv^2\gg\frac{1}{2}mV^2=\frac{1}{2}(m/M)MV^2$ or $E\gg(m/M)E_{\rm rot}$, where $E_{\rm rot}\simeq\frac{1}{2}MV^2$ is the molecular rotational kinetic energy. Even in the lightest molecule (H_2), this admittedly crude condition (if only because the electron velocity in the vicinity of the molecule may differ from its velocity at infinity) merely requires $E\gg10^{-4}$ eV, as was stated in Sec. 1. We stress that this energy criterion for the validity of the fixed-nuclei approximation is sensible only for calculations of purely elastic scattering amplitudes.

The first applications of the fixed-nuclei model were carried out by Stier (1932) and Fisk (1936). An outline of their treatment is as follows: Introduce ellipsoidal (or prolate spheroidal) coordinates [Magnus and

Oberhettinger, 1949], defined by the coordinates μ and λ (Fig. 37).

$$\lambda=(r_A+r_B)/R_{AB}, \qquad \mu=(r_B-r_A)/R_{AB}$$
$$1\leq\lambda\leq\infty \qquad -1\leq\mu\leq 1. \tag{4.1}$$

In a sense, μ is the generalization of the quantity $\cos\theta$ in spherical coordinates, where θ is the polar angle of the electron relative to the internuclear axis; specifically $\mu\rightarrow\cos\theta$ as $R_{AB}\rightarrow 0$, or as $r_A, r_B\rightarrow\infty$.

The interaction between the incident electron and the molecular nuclei (charge Z) is

$$V_e=-(2Z/r_A)-(2Z/r_B)=-(8Z/R_{AB})[\lambda/(\lambda^2-\mu^2)], \tag{4.2a}$$

where we have introduced atomic units (r_A, r_B in units of the Bohr radius; energy in units of the Rydberg). With this interaction, the Schrödinger equation for the incident electron is separable in prolate spheroidal coordinates (the reason for introducing these coordinates, of course), as is well known from the theory of the hydrogen molecular ion (Pauling and Wilson, 1935). The idea of the Stier–Fisk model is to add an interaction resembling the repulsion of the incident electron by the molecular electrons, but without disturbing the separability of the Schrödinger equation. This can be done by introducing, instead of (4.2a), the interaction

$$V=-\frac{8Z}{R_{AB}}\frac{\lambda}{\lambda^2-\mu^2}\left[1-\frac{\lambda_0}{\lambda}\frac{(\lambda-1)^2}{(\lambda_0-1)^2}\right] \qquad \lambda\leq\lambda_0$$
$$V=0 \qquad \lambda>\lambda_0. \tag{4.2b}$$

Physically, the added factor (in brackets) in (4.2b) has the effect of distributing the positive charge throughout the volume of the ellipsoid, while simultaneously reducing the potential outside to zero. By implication, therefore, the model puts a layer of negative charge on the surface in order that the potential be zero outside. Evidently, the model is crude compared to a real molecule, not to mention the fact that exchange of the scattered and orbital electrons is not at all included. But there is at least one free parameter, namely the boundary ellipsoid λ_0, by which one can hope phenomenologically to make up for the aforementioned deficiencies; also, the effective charge Z can be adjusted to fit other atomic data. At any rate, even in this very rudimentary form the fixed-nuclei model yields total electron–molecule scattering cross sections of the right order of magnitude, as can be seen from Figs. 10, 12, and 16. Concentrating on Fig. 16 for e^-–H_2, we observe that the experimental results of Ramsauer and Kollath (1930), and of Golden, Bandel, and Salerno (1966), are reasonably well accommodated below 5 eV by Fisk's fit.[28] Above 5 eV his theoretical cross sections are definitely too low; in this energy range the more sophisticated calculations (Fig. 25) by Lane and Geltman (1967) discussed in Sec. 3 are a distinct improvement on Fisk's. On the very low-energy side (energies $<\sim$1 eV), Fisk's results are definitely too high, and, going in the wrong direction, a feature also manifested by Lane and Geltman's (1967) theoretical results (Fig. 25).

These low-energy failures of the theory presumably are to be ascribed to the neglect of electron exchange in Fisk's and in Lane and Geltman's calculations (as was discussed in Sec. 3). Actually, it took over twenty years beyond Fisk's calculations to demonstrate that exchange is important in electron–molecule collisions, although even before Fisk the profound effect of exchange in electron–atom scattering had been shown by Morse and Allis (1933). This demonstration—of the effect of exchange on e^-–H_2 total cross sections—was first given by Massey and Ridley (1956). They employed the completely antisymmetrized form

$$\Psi(1,2,3)=\sum F(\mathbf{r}_i)\Phi(\mathbf{r}_j,\mathbf{r}_k)\chi_i^+(\chi_j^+\chi_k^--\chi_j^-\chi_k^+) \tag{4.3}$$

to obtain the wave function Ψ approximately solving Schrödinger's equation for e^-–H_2 scattering. The sum in (4.2) is over the three independent cyclic permutations of the subscripts i, j, k designating the three electrons 1, 2, 3 in the system. The term written explicitly in (4.2) corresponds to electron i incident, with j, k the molecular electrons; $\chi_\pm$ are the usual single-particle spin 1/2 eigenfunctions. The spatial part of the target molecular ground-state eigenfunction employed by

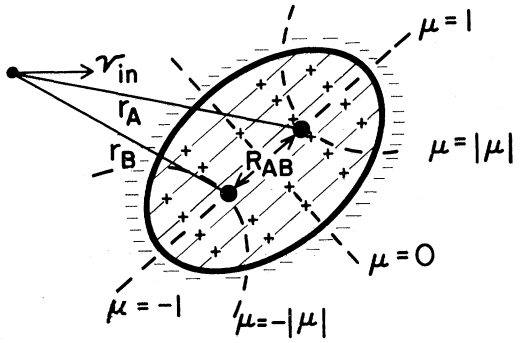

FIG. 37. Ellipsoidal coordinates for electron–molecule scattering calculations. R_{ab} is the internuclear distance. r_A, r_B are the distances from the individual nuclei to the incident electron, speed v_{in}. Lines of fixed μ are dashed. The heavy black ellipse is a curve of constant $\lambda=\lambda_o$. The Stier–Fisk model assumes the potential is zero outside this boundary. The shading and + signs indicate that on this model the nuclear charge is supposed to be distributed throughout the volume bounded by the ellipsoid $\lambda=\lambda_o$.

[28] Fisk's work—especially his use of a spheroidal expansion and his introduction of a separable potential—was based on procedures developed by Morse (1935). A similar spheroidal expansion was independently employed by Kotani, references to whose work may be found in Nagahara (1953, 1954).

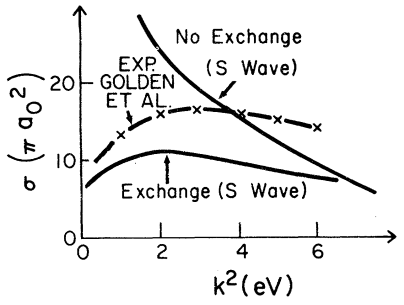

FIG. 38. Effect of including exchange integrals. Theoretical curves, from Massey and Ridley (1956); experimental curve, from Golden, Bandel, and Salerno (1966).

Massey and Ridley was

$$\Phi(j,k)=w(j)w(k)$$
$$w(j)=N\exp(-q\lambda_j)(1+f\mu_j^2+g\lambda_j) \quad (4.4)$$

from Coulson (1938); here q, f, g are known constants, and μ_j, λ_j are the spheroidal variables (referring to the jth electron) defined in (4.1).

Massey and Ridley then were able to calculate the "S-wave" scattering phase shift η_{00} from the asymptotic form of F in (4.3), namely from

$$F(\mathbf{r}_i)=1/(1+a^2)^{1/2}-[c(\lambda_i-1)]^{-1}$$
$$\times(\sin c(\lambda_i-1)\{a+b\exp[-\gamma(\lambda_i-1)]\}$$
$$\times\{1-\exp[-\gamma(\lambda_i-1)]\}\cos c(\lambda_i-1)) \quad (4.5a)$$
$$\to\sin(c\lambda_i+\eta_{00})/c\lambda_i \qquad \lambda_i\to\infty \quad (4.5b)$$

where a, b, and γ are as yet undetermined constants, and

$$c=\tfrac{1}{2}kR_{AB}, \quad (4.5c)$$

with k the wave number of the incident electron (in atomic units). The "best" values of a, b, and γ were found using the Kohn (1948) variational principle. In the Kohn principle, one varies the expression

$$L=\int\Psi(H-E)\Psi, \quad (4.6a)$$

where Ψ is the purported solution (4.3) to Schrödinger's equation, satisfying the required boundary conditions. Using (4.3), Massey and Ridley rewrote (4.6a) in the form

$$L\equiv L_D+L_E, \quad (4.6b)$$

where L_D involved only direct (nonexchange) integrals, and L_E involved exchange integrals only. When Massey and Ridley kept only L_D, the resultant "S-wave" phase shift was such as to give a huge low-energy cross section, reminiscent of the Fisk result and in gross disagreement with experiment. With retention of L_E, however, the cross section is lowered dramatically, as shown in Fig. 38 (the exchange curve of Fig. 38 is a replot of the curve labeled Massey and Ridley in Fig. 36). Thus for the *first time* one could say that a fundamental (not semiempirical via introduction of adjustable parameters to fit some of the data) electron–molecule collision calculation was in semiquantitative agreement with experiment. In detail, introducing exchange causes the Massey and Ridley e^-–H_2 zero-energy phase shift to approach π rather than zero radians, as typically occurs in e^-–atom scattering; the concomitant reduction—by inclusion of exchange—of their e^-–H_2 cross sections near the elastic threshold also is analogous to frequently observed exchange effects in e^-–atom collisions. Finally, the exchange cross section in Fig. 38 is rather flatter at low energies than is the experimental curve. This is a well-known defect of the exchange approximation in e^--atom scattering, and indicates the need for inclusion of induced polarization effects; similar behavior of calculations including exchange but omitting polarization can be seen in the no-polarization curves of Fig. 36 [one of which is the Tully and Berry (1969) curve].

The calculation of Massey and Ridley can be regarded as the first quantitative calculation of e^-–H_2 scattering cross sections. The next step in improving the accuracy is to include higher partial waves. To do this in spheroidal coordinates, while at the same time retaining the electron–electron interaction as did Massey and Ridley, one must go beyond the separable spheroidal analysis of Stier and Fisk. This was in fact done first by Nagahara (1953), but his calculations (Nagahara, 1954) for e^-–H_2 scattering did not include exchange, and any agreement with experiment his results may contain now is generally considered to be coincidental. The nonseparable spheroidal analysis has been repeated more recently by Takayanagi (1967) and by Hara (1969a). The latter has gone much further, in that he actually has done the calculation including polarization as well as exchange.

We shall discuss Hara's results in due course. For the moment, however, let us note a disadvantage of spheroidal analysis, namely that the spheroidal harmonics in terms of which the scattering amplitude is expressed (Morse and Feshbach, 1953) depend on the internuclear distance, R_{AB}, of the particular molecule being investigated. This means that the experimentalist would infer different scattering parameters for different molecules (having presumably different R_{AB}'s) even if their observed scattering rates were the same. Not only is this inconvenient, but it is really unphysical, because the internuclear separation is something which isn't observed in the scattering experiment at all. If we made the analysis in terms of the more customary spherical harmonics, this problem would not arise.

4.11 Single-Center Expansions

Therefore, we now shall examine the description of electron–molecule scattering in terms of an expansion in spherical harmonics, instead of in the (at first sight more physical) spheroidal expansion associated with the spheroidal coordinates (4.1). A single-center spherical harmonic expansion for electron–molecule collisions first was systematically employed by Temkin

and Vasavada (1967), whose work was extended in Temkin, Vasavada, Chang, and Silver (1969). In Fig. 39, we sketch the electron–molecule collision geometry relevant to a single-center expansion. We introduce a rectangular system of coordinates in the laboratory frame, with the laboratory z direction (along $\hat{\mathbf{z}}'$) parallel to the initial velocity $\mathbf{v}$ of the incident electron. The molecular internuclear axis still is assumed fixed, and points along $\hat{\mathbf{z}}$; associated with $\hat{\mathbf{z}}$ are a set of $\hat{\mathbf{x}}$ and $\hat{\mathbf{y}}$ axes (not shown) fixed in the molecular frame. The orientation of the molecular frame relative to the laboratory frame is specified by three Eulerian angles, defined as usual (Goldstein, 1965); these Eulerian angles are designated by the single symbol β_0 in Fig. 39. The instantaneous position of the electron relative to the center of the internuclear axis is $\mathbf{r}$; the incident electron ultimately will be scattered into the direction specified by Ω' in the laboratory frame.

In terms of the above coordinates, the (total elastic) scattering amplitude at a given incident energy can be designated by $f(\beta_0, \Omega')$, expressing the fact that the scattering amplitude in general depends on the orientation β_0 of the molecule, as well as on the direction Ω' of the outgoing electron. The following simplifying observations can be made, however. In the approximation that the internuclear axis is fixed, writing the Schrödinger equation in terms of unprimed ($\hat{\mathbf{z}}$ along the internuclear axis) coordinates is just as valid as writing the Schrödinger equation in terms of the original primed ($\hat{\mathbf{z}}'$ along $\mathbf{v}$) laboratory coordinates. But in the unprimed coordinate system, the Hamiltonian—though it depends on the x, y, z coordinates of the incident electron, of course—is quite independent of the direction along which the electron is initially incident. Moreover, if the incident direction $\mathbf{v} \parallel \hat{\mathbf{z}}$ and the final direction Ω' are rotated together, and if the same rotation then is performed on the unprimed molecular frame relative to the laboratory frame, the scattering amplitude $f(\beta_0, \Omega')$ obviously cannot change. Taking these simplifying observations into account, it can be shown that $f(\beta_0, \Omega')$ has the "factored" expansion

$$f(\beta_0, \Omega') = \sum_{m,m'} \sum_{l_i l_j} a_{l_i l_j m} \mathfrak{D}_{m'm}^{(l_i)}(\beta_0) \mathfrak{D}_{0m}^{(l_j)*}(\beta_0) Y_{l_i m'}(\Omega'), \quad (4.7)$$

where the $Y_{l_i m'}$ are the usual spherical harmonics; the $\mathfrak{D}$ functions, the so-called rotational harmonics (Edmonds, 1957), are known functions of β_0; and the $a_{l_i l_j m}$ are numbers, determined by the particular electron–molecule interaction, but independent of β_0.

Thus, via the expansion (4.7), for each molecular target at each energy, the dynamical problem can be solved for the numbers $a_{l_i l_j m}$ once and for all, and the dependence on β_0 then simply multiplies those numbers by factors. In addition to its simplicity, this feature of (4.7) will be seen to have important implications for the adiabatic-nuclei theory of rotational excitation discussed in the next subsection. Furthermore, in the approximation wherein the various partial waves are

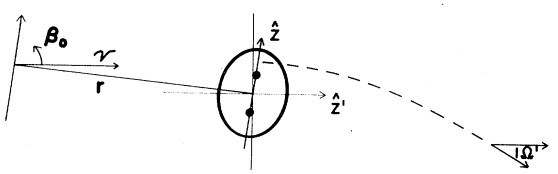

FIG. 39. Geometry for single-center expansion. The z direction in the laboratory frame is $\mathbf{z}'$, parallel to the initial velocity $\mathbf{v}$ of the incident electron. The incident electron's position relative to the molecular center is $\mathbf{r}$. The electron will scatter into the direction defined by Ω' in the laboratory frame. The single symbol β_0 designates the orientation of rectangular axes fixed in the molecular frame relative to axes fixed in the laboratory frame; the z direction in $\hat{\mathbf{z}}$ the molecular frame lies along the internuclear axis.

supposed to be uncoupled, an approximation which turns out to be an excellent one in many cases, the $a_{l_i l_j m}$ reduce to a very familiar form involving phase shifts η_{lm}, namely

$$a_{l_i l_j m} \longrightarrow \delta_{l_i l_j}\{[4\pi(2l_i+1)^{1/2}/k]\} \exp(i\eta_{lm}) \sin \eta_{lm}.$$

In this approximation it is quite obvious what price we have paid for eliminating β_0 from the dynamical problem—the η_{lm} depend on the magnetic quantum number m as well as on l. Generally this is a small price to pay, as we shall see when we look at some radial equations. We add that the consistency of the procedure starting with the expansion (4.7) is evinced by the fact that the optical theorem holds for all angles of orientation β_0 (Temkin, Vasavada, Chang, and Silver 1969).

In summary, the single-center spherical harmonic partial-wave expansion can be carried out consistently even for the spherically nonsymmetric targets occurring in electron–molecule collisions; moreover, this expansion in principle yields a complete description of the collision. In practice, however, the expansion must be truncated, and we still must inquire into its pragmatic utility. In order that the single-center expansion converge reasonably rapidly, the incident electron should not be able to penetrate into the molecular core. The basis for this assertion is the sketch (solid line in Fig. 40) of the potential energy $V(\mathbf{r})$ of an electron in the vicinity of the nuclei. The potential becomes singular only on a single line through the origin, namely the internuclear axis, and this very pronounced deviation from spherical symmetry means [recall Fig. 37 and Eq. (4.2a)] that the spherical harmonic expansion of $V(\mathbf{r})$

$$V(\mathbf{r}) \equiv V(r, \theta, \varphi) = -(2/r_A) - (2/r_B) = \sum_l V_l(r) P_l(\cos\theta) \quad (4.8)$$

will converge only very slowly at $r \sim \frac{1}{2}R_{AB}$; in (4.8), the interaction obviously is azimuthally symmetric about the internuclear axis, i.e., depends only on r and on the angle θ between $\mathbf{r}$ and $\hat{\mathbf{z}}$ (Fig. 39). The lowest order V_0 term on the right side of (4.8) is sketched as the dashed line in Fig. 40, and obviously is indeed a crude approximation to $V(\mathbf{r})$ in the vicinity of $z=$

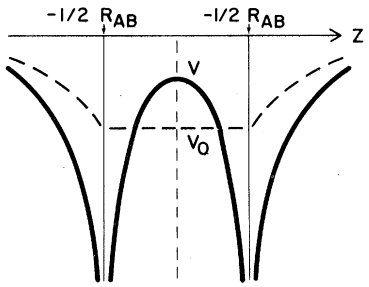

FIG. 40. Electron–molecule interaction on the internuclear axis. Solid line, actual interaction $V(\mathbf{r})$; dashed line, lowest order term $V_0(\mathbf{r})$ in the spherical harmonic expansion of $V(\mathbf{r})$.

$\pm\frac{1}{2}R_{AB}$ ($r=\frac{1}{2}R_{AB}$, $\theta=0$ and π). In contrast to the spherical expansion, then, the real advantage of spheroidal coordinates is *not* that they simplify the partial wave analysis (they do not, in fact as noted above they are interpretatively further removed from experiment). But spheroidal coordinates do allow the singularities in $V(\mathbf{r})$ near the nuclei to be included in a natural way.

The considerations of the preceding paragraph make it clear that there will be no simple criterion for the accuracy (i.e., reasonably rapid convergence, permitting practical truncation) of the spherical harmonic expansion. If, for example, the effective wave number of the electron near the nucleus is much larger than the wave number k at ∞, the most obvious criterion, namely that $kR_{AB}\ll 1$, may not prevent s and higher partial waves from probing the molecular core; in this event, a severely truncated expansion will be inadequate. Even if only the s wave penetrates the molecular core, the expansion may be invalid because of the aforementioned fact that $V_0(r)$ is so poor a representation of $V(r)$. The upshot of these remarks is that probably we will be able to evaluate the utility of the single-center expansion in electron–molecule scattering only by actually using it and then comparing its predictions with experiment. We proceed, therefore, to examine the results of actual single-center expansion calculations.

In this connection, for historical reasons, we first mention the single-center calculation of Carter, March, and Vincent (1958). Their calculation was extremely crude, and exchange was taken into account only in an approximate way. Nevertheless, this was the first single-center electron–molecule scattering calculation, and it supported the conclusion of Massey and Ridley (1956) that exchange was essential for reduction of the low-energy elastic cross section. Unfortunately, Carter, March, and Vincent (1958) did not wholly correctly take into account the rotational symmetry of $f(\boldsymbol{\beta}_0, \boldsymbol{\Omega}')$—expressed by the expansion (4.7)—so that they inferred the phase shifts must depend on $\boldsymbol{\beta}_0$, a very misleading conclusion.

4.12 Calculations using Spherical Harmonic Expansions

We next turn to the work of Temkin and Vasavada (1967) on e^-–H_2^+ collisions, which of course are even simpler than collisions of electrons with H_2. We shall confine our attention to the uncoupled approximation described in subsection 4.11. In practice, this approximation means we are confining our attention to s and p waves; for the phase shifts of $l\geq 2$ waves, coupling to the lower order s and p waves occurs. The two-electron wave function $\Psi(1, 2)$ solving the Schrödinger equation for e^-–H_2^+ collisions in the present approximation takes the form

$$\Psi(1, 2)=\sum_{lm}\Psi_{lm}{}^{(N)}, \tag{4.9}$$

where Ψ_{lm} is the wave function for the lmth partial wave in the Nth order of approximation. The expression for $\Psi_{lm}{}^{(N)}$ [excluding spin functions] is

$$\Psi_{lm}{}^{(N)}=[u_{lm}(r_1)/r_1]Y_{lm}(\boldsymbol{\Omega}_1)$$
$$\times[\Phi_0{}^{(N)}(\mathbf{r}_2)+\Phi_0{}^{(POL)}(\mathbf{r}_1;\mathbf{r}_2)]\pm(1\rightleftarrows 2). \tag{4.10}$$

The last term in (4.10) denotes the appropriate symmetrization of the more explicitly detailed preceding terms, wherein one can suppose that electron 1 is incident and electron 2 is bound; the + and − signs refer to singlet and triplet scattering respectively. In further explanation of (4.10), the u_{lm} are radial functions, determined by Eqs. (4.13) below; $\boldsymbol{\Omega}_1$ designates the instantaneous direction (specified by the spherical coordinate angles θ_1, ϕ_1) of the position vector $\mathbf{r}_1$ locating electron 1 in the unprimed internuclear frame of Fig. 39. Furthermore, the functions $\Phi_0{}^{(N)}$ and $\Phi_0{}^{(POL)}$ in (4.10) are to be regarded respectively as the unpolarized and polarized parts of the target H_2^+ wave function, in analogy to the corresponding functions arising in the method of polarized orbitals, that has been extensively used in electron-atom collisions (Temkin and Lamkin, 1961).

If the expansion did not have to be truncated, the unpolarized part of the target wavefunction would be known a priori; namely in e^-–H_2^+ collisions, this unpolarized part without truncation [termed $\Phi_0{}^{(\infty)}$] would be the wavefunction of H_2^+ in its ground Σ_g state, and would have the expansion

$$\Phi_0{}^{(\infty)}(\mathbf{r}_2)=\sum_{n=0}^{\infty}{}''\frac{\varphi_n{}^{(\infty)}(r_2)}{r_2}P_n(\cos\theta_2), \tag{4.11a}$$

where the double prime on the summation symbol indicates that n takes on even values only (in the present H_2^+ case the symmetries of homonuclear diatomic molecules causes the odd n terms to vanish). The ($\frac{1}{2}N$th order) approximation to $\Phi_0{}^{(\infty)}$ is $\Phi_0{}^{(N)}$ in (4.10), whose expansion is taken to be

$$\Phi_0{}^{(N)}(\mathbf{r}_2)=\sum_{n=0}^{N}{}''\frac{\varphi_n{}^{(N)}(r_2)}{r_2}P_n(\cos\theta_2). \tag{4.11b}$$

The radial functions $\varphi_n{}^{(N)}(r_2)$ in (4.11b) are the "best" for given $N<\infty$; specifically, $\varphi_n{}^{(N)}$ are chosen so as to minimize the energy of H_2^+ for the expansion (4.11b) terminating at the given N. In practice, the difference between $\varphi_0{}^{(0)}$ and $\varphi_0{}^{(2)}$ was very small, and $\varphi_2{}^{(2)}(r)$ was quite small compared to $\varphi_0{}^{(2)}(r)$ at all r of interest

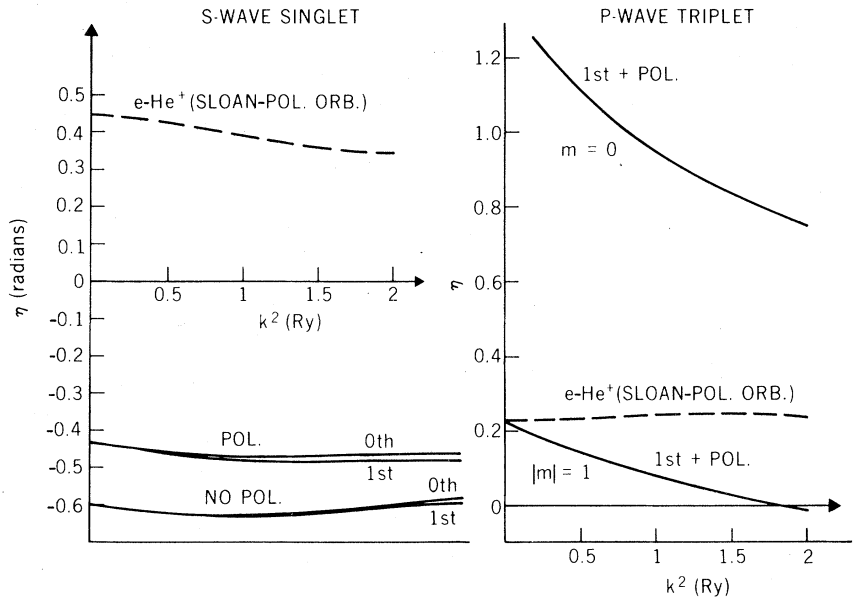

FIG. 41. Calculated phase shifts. Solid lines, e^-–H_2^+ phase shifts, computed via single-center expansions (Temkin and Vasavada, 1967); zeroth-order vs. first-order results are shown, as are the results of including or omitting polarization corrections. Dashed lines, e^-–He^+ atomic polarized orbital phase shifts (Sloan, 1964).

(Temkin and Vasavada, 1967). Thus the single-center expansions (4.11b) for the unpolarized (but nevertheless spherically nonsymmetric) part of the target wavefunction do converge reasonably rapidly, in e^-–H_2^+ collisions at any rate. In fact, Temkin and Vasavada's calculations (partial results are displayed in Fig. 41 below) did not go beyond the first order ($N=2$) corrections. In this circumstance, $\Phi_0^{(POL)}$ of (4.10) consistently can be written in the form (Temkin and Vasavada, 1967)

$$\Phi_0^{(POL)}(\mathbf{r}_1;\mathbf{r}_2) = -[\epsilon(r_1,r_2)/r_1^2] \times (\varphi_0^{(POL)}(r_2)/r_2)[\cos\theta_{12}/(4\pi)^{1/2}] \quad (4.12a)$$

where θ_{12} is the angle between $\mathbf{r}_1$ and $\mathbf{r}_2$; $\varphi_0^{(POL)}$ is determined solely by the lowest-order term $\varphi_0^{(0)}$ in (4.11a); and the step function $\epsilon(r_1,r_2)$ is defined by

$$\epsilon(r_1,r_2)=0 \qquad r_1<r_2$$
$$\epsilon(r_1,r_2)=1 \qquad r_1>r_2. \quad (4.12b)$$

The philosophy behind inclusion of only first-order polarization corrections $\varphi_0^{(POL)}$ in the expression (4.12a) for $\Phi_0^{(POL)}$ is essentially the same as the philosophy behind retention of only first order $N=2$ terms in (4.11b). In the latter case, the basic assumption is that the internuclear distance not be too large (i.e., that the molecule not be too aspherical); in the former case, the basic assumption is that the molecular polarizability not be too large. In both cases one cannot give an *a priori* limit as to what too large means [just as we were not able to set an a priori criterion for the utility of the spherical harmonic expansion (4.8)], but in practice it appears that one can be pretty liberal, at least for the lightest nuclei.

With the above expansion (4.11b) and (4.12a), the radial equations determining the radial functions u_{lm} in (4.10) are (with the understanding that $l=0$, 1 only)

$$\left(\frac{d^2}{dr^2} - \frac{l(l+1)}{r^2} + V_0(r) - \delta_{1l}\frac{(3m^2-2)}{5}V_2(r) - 2\int_0^\infty r_>^{-1}[\varphi_0^{(N)}(r_2)]^2\,dr_2 + \frac{2\delta_{l1}\delta_{N2}}{5^{1/2}}\left(\frac{3m^2-2}{5}\right) \times \int_0^\infty \frac{r_<}{r_>^2}\varphi_0^{(2)}\varphi_2^{(2)}\,dr_2\right) u_{lm}(r) \pm (\text{exchange terms})$$
$$= -\frac{2}{3}\frac{u_{lm}(r)}{r^4}\int_0^r r_2\varphi_0^{(N)}\varphi_0^{(POL)}\,dr_2 \pm (\text{exchange–polarization terms}), \quad (4.13a)$$

where

$$V_l(r) = 4r^l/(\tfrac{1}{2}R_{AB})^{l+1} \qquad r<\tfrac{1}{2}R_{AB}$$
$$= 4(\tfrac{1}{2}R_{AB})^l/r^{l+1} \qquad r>\tfrac{1}{2}R_{AB}; \quad (4.13b)$$

Here $r_>$, $r_<$ are respectively the greater or lesser of r_2 and r, δ designates the usual Kronecker symbol, and the various φ functions under the integral signs in (4.13a) depend on r_2, of course.

The radial equations (4.13) have been displayed to make explicit their similarity to the radial equations arising in the polarized orbital method for the collisions of electrons with atomic hydrogen (Temkin and Lamkin, 1961). On the right hand side of (4.13a), we see a direct polarizability term. The exchange and exchange–polarization terms (whose signs depend on the symmetrization) have not been written out in detail; they represent the difference between singlet and triplet scattering equations.

When we come to p waves ($l=1$), we see the first manifestation of the m dependence of the equations. In particular, from (4.13b) the V_2 term in (4.13a) is seen to behave like r^{-3} at infinity; this is the quadrupole

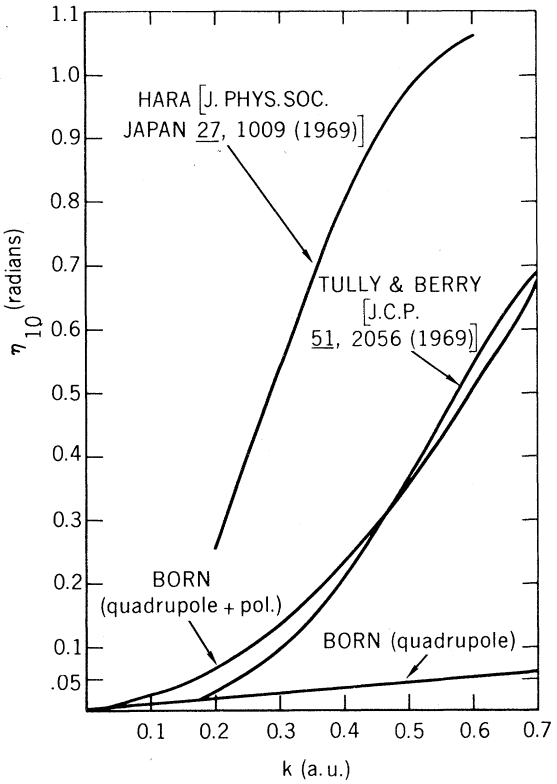

FIG. 42. P wave $m=0$ $^2\Sigma_u$ e^-–H_2 phase shifts, from Tully and Berry (1969), and from Hara (1969a). The Born approximation results, calculated for a pure quadrupole interaction with and without induced polarization, also are shown. The incident wave number k is in atomic units.

term, and it changes sign from attractive for $m=0$ to repulsive for $|m|=1$. To some extent these m-dependent quadrupole effects are opposed by the first-order correction; but since $|\phi_2^{(2)}| \ll |\phi_0^{(2)}|$ (as already pointed out), the modifications of the m dependence stemming from the first-order correction are not predominant.

The effects that have been discussed above are discernible in the numerical results obtained by Temkin and Vasavada (1967), some of which are shown in Fig. 41. On the left we see their ^1S phase shifts. Evidently, polarization effects are significant in these ^1S calculations; because induced polarization potentials are always attractive, including polarization algebraically increases the computed phase shifts. Also we see that first-order (nonspherical) effects are very small for these ^1S phase shifts. For comparison, we have added on the left of Fig. 41 a plot of the ^1S e^-–He^+ phase shifts computed by Sloan (1964) via the established polarized orbital procedures for electron–atom collisions (Temkin and Lamkin, 1961); in effect, He^+ is the single-center target that H_2^+ would become if its nuclei were to merge. One sees that the computed e^-–He^+ ^1S phase shifts are very much larger algebraically than the computed e^-–H_2^+ ^1S phase shifts; of course, in e^-–He^+ collisions, unlike e^-–H_2^+ collisions, the spherical expansion treatment Sloan employed takes full account of the singularity of the nuclear potential. Thus, the differences between the e^-–He^+ and e^-–H_2^+ curves on the left side of Fig. 41 give one some concern as to the quantitative accuracy of the single-center expansion in e^-–H_2^+ collisions, even though the first order corrections in e^-–H_2^+ were found to be small. However, the single-center He^+ target is sufficiently different from the two-center H_2^+ target that the deviations between e^-–He^+ and e^-–H_2^+ computed phase shifts cannot be regarded as disproving the accuracy of single-center calculations for e^-–H_2^+ collisions. A spheroidal calculation of e^-–H_2^+ scattering (which will test the single-center expansion) is being performed by A. B. Ritchie (unpublished).

On the right side of Fig. 41 are plotted some ^3P phase shifts. Again, previously discussed effects may be discerned. First, notice how the attractive quadrupole potential in the $m=0$ case increases that phase shift over the repulsive $|m|=1$ quadrupole potential. Second, note how large the $^3P_{m=0}$ phase shift is! It actually goes to about 80° at zero energy, a behavior which really has no counterpart even in the atomic case (dashed e^-–He^+ ^3P curve in Fig. 41). But this enhancement of the e^-–H_2^+ $^3P_{m=0}$ phase shift also cannot simply be described as a pure quadrupole effect. It was this circumstance which led to the suggestion (Temkin and Vasavada, 1967) that this e^-–H_2^+ enhancement might be associated with an H_2 counterpart of the $^2\Sigma_u^+$ compound state of H_2^-; this H_2^- resonance has been mentioned earlier, in connection with the measurements (Fig. 21) by Schulz and Asundi (1965) on H_2^- formation in e^-–H_2 collisions.

Without further ado, therefore, let us turn to the P-wave, $m=0$ $^2\Sigma_u$ e^-–H_2 phase shifts, shown in Fig. 42. In essence, the calculation of Tully and Berry (1969) includes exchange and the permanent distortion (from spherical symmetry) of the molecule, but does not include induced polarization[29] (as we already have mentioned). Because the induced polarization plus the long-range effects of permanent distortion (i.e., the quadrupole potential) can be included with moderate accuracy in the Born approximation for partial waves $l>0$, we include in Fig. 42 the Born P-wave $m=0$ phase shifts, computed on the assumption that the interaction between the incident electron and the unpolarized molecule is pure quadrupole.

If the polarization contribution (indicated by the Born curves in Fig. 42) is added to Tully and Berry's phase shifts, one gets results very close to the Hara (1969a) phase shifts plotted in Fig. 42. Hara has made the most complete calculation of e^-–H_2 scattering thus far. In addition to automatically taking account of

[29] The results of Tully and Berry (1969) supplant the calculation of Wilkins and Taylor (1967), who apparently incorrectly solved their equations. Many of Wilkins and Taylor's results are very similar to Tully and Berry's, and we believe the accurately solved Wilkins and Taylor equations would in all cases yield values very close to Tully and Berry's.

permanent distortion by using spheroidal coordinates, he has included polarization effects (Hara, 1969b). The only objection one might take to his important calculations is that it does not include the exchange polarization terms that would arise in a complete polarized orbital calculation. Cross sections inferred from Hara's calculations agree very well with experiment as already has been seen in Fig. 36, and as we shall illustrate in a moment.

The Hara $^2\Sigma_u$ results plotted in Fig. 42 indeed do manifest a pronounced enhancement of the P-wave $m=0$ phase shift, as Temkin and Vasavada (1967) had suggested would be the case; this enhancement in the e^-–H_2 P-wave $m=0$ phase shift (Fig. 42) really does correspond to the aforementioned similar enhancement in e^-–H_2^+ scattering (Fig. 41), although it happens that the e^-–H_2^+ phase shift peaks near zero energy (strictly a Coulomb effect) whereas the e^-–H_2 phase shift peaks near $k=0.6$ (about the energy of the experimentally observed peak in Fig. 21). Note, however, that Hara's $P_{m=0}$ phase shift does not pass through $\pi/2$ radians; thus to the extent that a "resonance" has been associated with this partial wave and with the Schulz and Asundi (1965, 1967) peak in Fig. 21 (Bardsley, Herzenberg, and Mandl, 1966), the term must be taken loosely. The word "resonance" carries implications concerning the shapes and maximum values of various partial cross sections which really don't accord accurately with e^-–H_2 experimental results. Furthermore, theoretically a resonance usually is associated with a specific kind of intermediate state, which dominates the process and must be included explicitly to make the phase shift increase by π radians. In actuality, no such state is included in Hara's calculation, and as we said, the phase shift does *not* increase by π radians. The augmentation certainly is present, but we would recommend our word "enhancement" for it; even the term "shape resonance" seems either too strong or too ambiguous.

4.2 "Adiabatic-Nuclei" Theory of Rotational Excitation

We next turn to the theory of rotational excitation. Obviously, rotational excitation is only possible if the nuclei actually are capable of rotation, i.e., we now must abandon the fixed-nuclei model which has been the primary subject of discussion thus far in this chapter. On the other hand, it remains true—as was explained earlier—that incident electron velocities v often are large compared to nuclear rotational velocities V. Hence, it should be possible to develop theories of rotational excitation for which the fixed-nuclei calculations serve as a starting point, recognizing that the range of validity of such rotational excitation calculations need not extend down to incident energies as low as 10^{-4} eV (recall Sec. 4.1). Indeed, such a theory has been developed; in fact the basic formula first was derived by Chase (1956) in the context of nuclear physics, where the problem was the excitation of deformed nuclei. Use of Chase's theory to compute rotational excitation customarily is termed the "adiabatic" theory of rotational excitation, because the nuclei are moving slowly compared to the incident electron. However, the term "adiabatic" here provides another illustration of confusing terminology; in the domain of atomic and molecular processes, an adiabatic collision between two bodies A and B normally is one in which the relative velocity of A and B is small compared to the velocities of their bound electrons. This certainly is the sense in which we employed the term "adiabatic" in the opening paragraphs of Sec. 3. For this reason, we prefer—and shall employ—the term "adiabatic-nuclei" for rotational excitation calculations based on Chase's work.

In the "adiabatic-nuclei" theory of rotational excitation, the amplitude $f_{\Gamma'\Gamma}(\mathbf{\Omega}')$ for scattering an electron into the laboratory direction $\mathbf{\Omega}'$ [recall Fig. 39], while simultaneously changing the rotational state of the molecule from initial state ψ_Γ to final state $\psi_{\Gamma'}$, is

$$f_{\Gamma'\Gamma}(\mathbf{\Omega}')\cong\int d\boldsymbol{\beta}_0\psi_{\Gamma'}^*(\boldsymbol{\beta}_0)f(\boldsymbol{\beta}_0,\mathbf{\Omega}')\psi_\Gamma(\boldsymbol{\beta}_0), \quad (4.14)$$

where $f(\boldsymbol{\beta}_0,\mathbf{\Omega}')$ is the scattering amplitude in the fixed-nuclei approximation, given by Eq. (4.7). There are two important observations to be made about this basic formula: First, use of the symbol $\cong$ indicates that the right-hand side of (4.14) does not yield the desired $f_{\Gamma'\Gamma}(\mathbf{\Omega}')$ exactly; there is an error which appears to be small when $v/V\gg1$, but whose precise order has not yet been definitively elucidated. Secondly, the analytic dependence of $f(\boldsymbol{\beta}_0,\mathbf{\Omega}')$ on $\boldsymbol{\beta}_0$, from (4.7), means that the integral (4.14) for $f_{\Gamma'\Gamma}$ can be evaluated analytically. For example, the total cross section (integrated over all angles $\mathbf{\Omega}'$) for excitation from j to j' is (Temkin and Faisal, 1971)

$$\sigma_{j'j}=(k_{\Gamma'}/k_\Gamma)\sum[a_{l\lambda m}a_{l\lambda\mu}^*/(2\lambda+1)]$$
$$\times\sum(-1)^{m+\mu}(l\lambda m-m\,|\,J0)\,(l\lambda\mu-\mu\,|\,J0)\,(jJ\Lambda-\Lambda\,|\,j'0)^2, \quad (4.15)$$

where the quantities in parentheses are Clebsch–Gordan coefficients; j,j' are the usual total orbital angular momentum quantum numbers labeling the rotational energy, in the rotational states fully labeled by Γ, Γ' respectively; k_Γ, $k_{\Gamma'}$ are respectively the initial and final electron wave numbers; Λ is the usual quantum number labeling the component (of the bound electrons' orbital angular momentum) along the internuclear axis, in the initial state Γ; and the sum in (4.15) runs over allowed values of l, λ, m, μ, J [for further details, see Temkin and Faisal (1971), and Chang and Temkin (1969)].

Chase himself did not reduce the integral (4.14) for $f_{\Gamma'\Gamma}$ to simplest terms, nor did he obtain the formula (4.15). Oksyuk (1966), who was one of the first[30] to

[30] Probably the first application to electron–molecule collisions was by Altshuler (1957), in his elegant Born approximation treatment (mentioned in chapter 1) of rotational excitation for molecules possessing a permanent dipole moment. See also Crawford *et al.* (1967).

apply Chase's theory seriously to electron–diatomic molecule collisions, did obtain useful expressions in the approximation that the partial waves (in the scattered electron's wavefunction) are uncoupled; it will be recalled that we have asserted this approximation—which was employed in deriving Eq. (4.13a)—often is excellent. However, the phase shifts Oksyuk used were derived from a calculation along the lines of Fisk (1936), discussed early in this chapter; therefore, Oksyuk's results, though occasionally qualitatively impressive, assuredly aren't quantitatively fundamental and can be quite misleading (recall Fig. 28). Mittleman, Peacher, and Rozsnyai (1968) applied Chase's theory to rotational excitation of polar (i.e., heteronuclear) molecules, but again their calculation did not utilize scattering parameters from a detailed fixed-nuclei calculation, but used rather a special soluble model due to Mittleman and von Holdt (1965). The adiabatic-nuclei cross sections in the full coupled form for homonuclear molecules in Σ states were worked out for neutrals by Chang and Temkin (1969), and for charged targets (molecular ions) by Chang and Temkin (1970). Independently, Hara (1969c) has derived the necessary formulae, and has applied the adiabatic-nuclei theory to his spheroidal calculation of e^-–H_2 scattering. Finally, Temkin and Faisal (1971) have derived the generalized formulae for non-Σ states.

Three implications of (4.15) should be noted. First, for a rotational transition ($j \neq j'$), the final Clebsch–Gordan coefficient in (4.15) vanishes unless $J \neq 0$; while if $J \neq 0$, the first two Clebsch–Gordan coefficients in (4.15) imply that *both* l and λ cannot be zero. But the symbols l, λ refer to the orbital angular momenta of the outgoing and incident electron respectively. Thus, (4.15) shows that pure s-wave parameters (s waves in and s waves out) do not contribute to rotational excitation or deexcitation, as is obvious on grounds of angular momentum conservation. Since exchange effects are most important in s waves, these remarks may explain why a model as crude as Stier–Fisk's, when used in the "adiabatic-nuclei" formalism (Oksyuk, 1966) can yield results which—if not wholly correct—at least are not wrong by orders of magnitude.

Secondly, when $\Lambda = 0$ (Σ states) in (4.15), it is known (Gerjuoy and Stein, 1955a) that $\sigma_{T'T} = 0$ for $\Delta j = |j' - j| =$ an odd integer. Basically, this selection rule expresses the fact that the rotational transition is being caused by an even (at long range, quadrupole) interaction, while the parities of Σ rotational states alternate, starting from the lowest $j = 0$ level. Formally, the selection rule is deduced from (4.15) via the relationship $a_{l\lambda m} = a_{l\lambda,-m}$ valid for homonuclear targets (Temkin *et al.*, 1969). It is to be emphasized, however, that in the general case ($\Lambda \neq 0$), the ($\Delta j =$ even integer only) selection rule no longer holds (Temkin and Faisal, 1971). In essence, the selection rule does not obtain when $\Lambda \neq 0$ because in this circumstance there are levels of even parity and of odd parity at every j, the so-called Λ-doubling phenomenon (Herzberg, 1950). Failure of the selection rule $\Delta j =$ odd integer for $\Lambda \neq 0$ also is associated with the fact that the well-known alternation of intensities in the band spectra of homonuclear molecules is not observed in transitions between states of $\Lambda \neq 0$, if the Λ-doubling cannot be resolved (Herzberg, 1950).

Thirdly, we point out that if (4.15) is summed over all final states j', one arrives at an expression σ_T which not only is independent of j, the initial state of rotation, but which actually is identical to the fixed-nuclei expression for elastic scattering averaged over classical directions of the internuclear axis (Temkin, Vasavada, Chang, and Silver, 1969). Specifically, we have

$$\sigma_T = \sum_{j'} \sigma_{j'j} = \sum_{l,\lambda,m} [\,| a_{l\lambda m} |^2/(2\lambda+1)\,] \rightarrow (4\pi/k^2) \sum_{l,m} \sin^2 \eta_{lm}. \tag{4.16}$$

The arrow in (4.16) indicates the final form of σ_T in the uncoupled approximation. It is in this way, then, that one finally learns precisely what is meant physically by elastic scattering in the fixed-nuclei approximation: it is the sum over all rotational states [starting from *any* fixed initial rotational state] of the scattering cross sections computed in the adiabatic-nuclei approximation. This result is very understandable, and was the basis for the remarks made in Sec. 3 in connection with Fig. 26.

A word is in order concerning threshold behavior and the adiabatic-nuclei theory. Strictly speaking, the error term in the adiabatic-nuclei approximation [the difference between the left and right sides of (4.14)] is energy dependent. The error can be minimized by applying the adiabatic-nuclei theory intelligently (Chang and Temkin, 1970) but there is no way of avoiding it altogether. At the threshold for rotational excitation, the outgoing electron is moving *slowly* even compared to the nuclear velocities, and the adiabatic-nuclei approximation is not justified. Right at threshold, therefore, the correct way of finding the cross section behavior is via the theory of Gerjuoy and Stein (1955). However, Chang and Temkin (1970) concluded that the adiabatic-nuclei theory becomes valid when the impacting electron energy exceeds approximately twice the rotational energy difference ΔE, in fact when

$$k_{inc}^2 > 1.65(\Delta E) \tag{4.17}$$

in atomic units. This criterion (4.17) for the validity of the adiabatic-nuclei approximation implies it is useable at considerably lower energies than previously had been estimated (Oksyuk, 1966; Hara, 1969c); the criterion also is supported by a close coupling calculation of Henry and Lane (1971). The Gerjuoy–Stein cross section, which is directly proportional to the quadrupole moment, beautifully accounts for the observed threshold behavior of the e^-–H_2 rotational excitation

cross section (Crompton, Gibson, and McIntosh, 1969), as Figs. 28 and 33 taken together show. In fact, the comparison of Crompton, Gibson, and McIntosh's results with the Gerjuoy–Stein theory near threshold yields a molecular H_2 quadrupole moment $Q=0.48\pm 0.01ea_0^2$ (Chang, 1970), in remarkable agreement with the theoretical value $Q=0.4858$ calculated by Karl and Poll (1967). By 0.2 eV above threshold, however, the Gerjuoy–Stein theory is low by a factor of 2 in e^-–H_2 rotational excitation; the augmentation in the experimental cross section is correctly predicted by the adiabatic-nuclei theory, and is accounted for by the enhancing $^2\Sigma_u$ (i.e., P-wave $m=0$) phase shift.

The threshold behavior for charged molecular targets (H_2^+) presents an interesting contrast to the foregoing. In an average sense the adiabatic-nuclei theory here can be applied down to threshold. (Chang and Temkin, 1970); in fact, most of the results can be obtained from the Coulomb–Born approximation (Stabler, 1963). On the other hand, e^-–H_2^+ is a case where rotational close coupling definitely would predict a series of resonances on top of the smooth background computed via the adiabatic-nuclei approximation. These resonances come from the strong coupling of the different rotational states in the presence of the electronic effects of the long range Coulomb tail. Fortunately, with the use of a coupled channel quantum defect formalism, these resonances conveniently can be parametrized in terms of the quantum defects of the *lower* $np\pi$ and $np\sigma$ orbitals of the compound system (H_2), together with their corresponding dipole moments and the rotational energy constant of the target (H_2^+) (Fano, 1970). The significant point is the behavior of the electron in the field of the H_2^+, wherein it is alternately repelled from the lower rotational state and attracted to the upper rotational, so that the lifetime in the vicinity of the target at a discrete set of energies is long and not short. Thus the electron in e^-–H_2^+ collisions fundamentally violates a presumption of adiabatic nuclei theory, namely that the nuclei change their orientation only very slightly during the collision [otherwise one hardly could compute $f_{\Gamma'\Gamma}$ in (4.14) using the fixed-nuclei scattering amplitude $f(\boldsymbol{\beta}_0, \boldsymbol{\Omega}')$]; in other words, the adiabatic-nuclei theory does not apply to e^-–H_2^+ collisions at these energies, and it is not surprising that one finds a series of resonances which are not predicted by the adiabatic nuclei formalism. From this e^-–H_2^+ case we learn that the semiclassical criterion for the validity of the adiabatic-nuclei approximation—namely that the incident (and outgoing) electron velocity v be large compared to the nuclear velocities V—provides no guarantee that the adiabatic-nuclei approximation will be successful. The adequacy of the adiabatic-nuclei theory, as well as of the fixed-nuclei approximation for that matter, to some extent can be decided only a posteriori.

Very near threshold, where the outgoing electrons are very slow (s waves), the rotational excitation cross section must be dominated by incoming d waves; this is the energy region where the Gerjuoy–Stein formula is valid. As the energy increases, the rotational excitation begins to be dominated by p waves (p in and p out), and the Gerjuoy–Stein theory becomes inferior to the adiabatic-nuclei theory, as has been explained. The importance of the p-waves can be seen from the following approximate formulas for inelastic differential cross sections deduced (Chang and Temkin, 1969) from the adiabatic-nuclei theory neglecting coupling between s and d waves

$$d\sigma_{j'j}/d\Omega' \cong [(j200 \mid j'0)^2/k^2] \times \{c_1[P_0(\cos\theta')+\tfrac{1}{5}P_2(\cos\theta')]+c_2(P_1+\tfrac{3}{7}P_3)\}, \tag{4.18a}$$

where

$$c_1 \cong \tfrac{2}{3}\sin^2(\eta_{10}-\eta_{11}),$$

$$c_2 \cong \tfrac{4}{5}\sin(\eta_{10}-\eta_{11})\sin(\eta_{20}+\eta_{21}-2\eta_{22}) \times \cos(\eta_{10}+\eta_{11}-\tfrac{2}{3}\sum_m \eta_{2m}). \tag{4.18b}$$

Indeed, Eqs. (4.18) show that primary importance attaches to the differences between the $\mid m \mid = -1, 0, 1$ components of the p wave, a result which readily can be understood; the m dependence is being caused by a spherically nonsymmetric interaction, which simultaneously is applying the torque to the nuclei.

Granted the p wave is dominant in rotational excitation and the s–d coupling is small, the angular distribution of the outgoing electron should show relatively little asymmetry about 90°, because this asymmetry is caused solely by interference between the p and d partial waves, and the d-wave phase shifts are small. Figure 43 compares theoretical and observed angular distributions, for the $j=1\rightarrow 3$ transition in e^-–H_2, at an energy of 4.42 eV (almost identical with the energies of the curves plotted in Fig. 30 for the same transition). The data points[27] in Fig. 43 are a replot of the rotational excitation (upper) points in Fig. 30; the Lane and Geltman (1969) curve in Fig. 43 (dash dot) is a replot of the rotational excitation (upper) curve in Fig. 30. However, in Fig. 43, we show some additional theoretical angular distributions for the e^-–H_2, $j=1\rightarrow 3$ transition. Note, first of all, that the data, and all the theoretical curves, manifest relatively little asymmetry about 90°, as was anticipated above. Next note the solid curve in Fig. 43, which really is a pretty fair fit[27] to the data points, considering their scatter. This curve was computed by Chang and Temkin (1969) in the following way. They obtained phase shifts by fitting the total (integrated over outgoing electron directions) rotational excitation cross sections of Ehrhardt and Linder (1968) and Crompton, Gibson, and McIntosh (1969), discussed in earlier chapters; the phase shifts so obtained then were used to compute the differential cross sections. In a sense, therefore, the agreement between the data points in Fig. 43 and the Chang and Temkin fit merely indicates the general

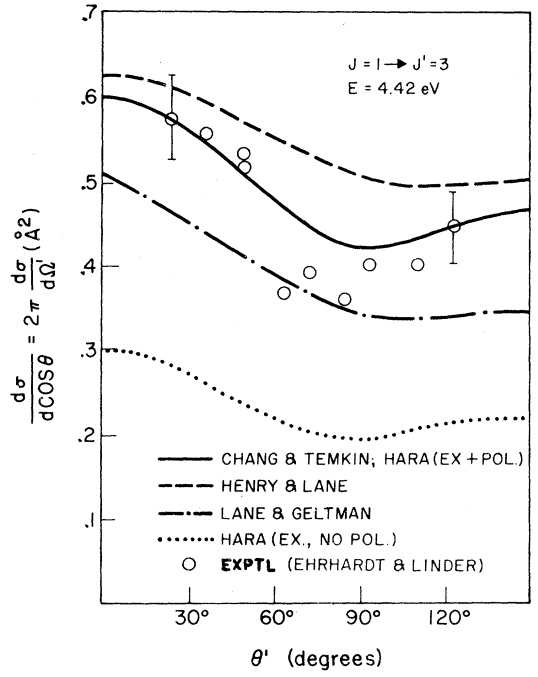

FIG. 43. Differential cross sections for outgoing electrons in e^-–H_2 scattering resulting in $j=1\rightarrow3$ rotational excitation. Circles, the measurements of Ehrhardt and Linder (1968). Solid line, theoretical calculations by Chang and Temkin (1969), and by Hara (1969c); Hara's slow-nuclei results include exchange and polarization. Dashed line, Henry and Lane (1969) close-coupling calculations, including exchange and polarization. Dotted line, Hara (1969c), omitting polarization. Dash–dot line, Lane and Geltman (1967, 1969) close-coupling calculation with semi-empirical polarization interaction and no exchange. See Footnote 27.

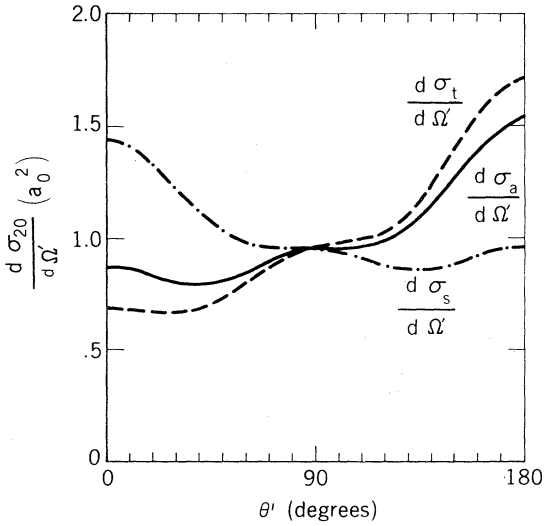

FIG. 44. Calculated differential cross sections for e^-–H_2^+ $j=0\rightarrow2$ rotational excitation at 6.8 eV. Dashed curve, $d\sigma_t/d\Omega'$, triplet scattering; dash–dot curve, $d\sigma_s/d\Omega'$, singlet scattering; solid curve, actually observable scattering, averaged over spin orientations.

consistency of measured e^-–H_2 rotational excitation differential and total cross sections; but the good fit also shows that the adiabatic-nuclei theory—whose formulas Chang and Temkin (1969) use in order to extract the phase shifts from the data—is basically correct. Of particular interest is the fact that the Chang and Temkin curve in Fig. 43—computed in this semi-empirical way—is indistinguishable from Hara's (1969c) wholly *a priori* predictions, which is another indication of the quality of his fixed-nuclei calculations (1969b). The lowest (dotted) curve in Fig. 43 is what Hara gets when he does not include polarization. The highest (dashed) curve in Fig. 43 represents the close coupling predictions of Henry and Lane (1969), including

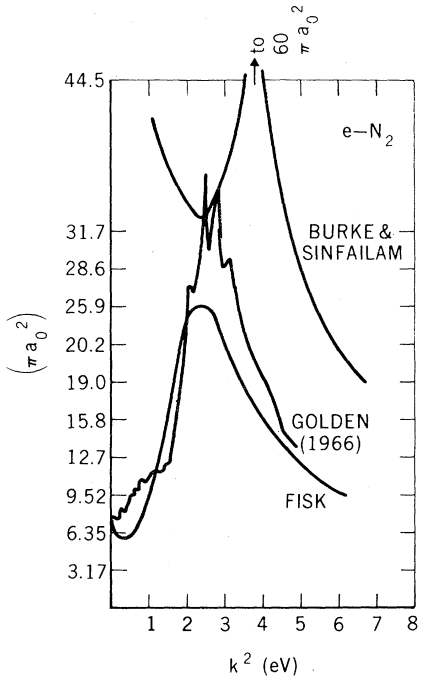

FIG. 45. Total scattering cross sections for e^-–N_2, from Burke and Sinfailam (1970), Golden (1966a), and Fisk (1936).

polarization and exchange; this dashed differential cross section curve corresponds to the solid Henry and Lane total cross section curve of Fig. 34.

The fairly close agreement in Fig. 42 between the adiabatic-nuclei results (Hara, 1969c) and the close-coupling results [Henry and Lane, 1969] when polarization and exchange are fully taken into account—and similar agreements noted in Sec. 3 [recall Fig. 36]—suggest that the adiabatic nuclei and close coupling theories of rotational excitation must be accurately related to each other by a unitary transformation. This transformation has been studied recently by Bottcher (1969); it does appear that aside from threshold effects and resonant behavior (recall the discussion earlier in this subsection), the two theories differ negligibly from each other.

Returning to the adiabatic-nuclei theory, in Fig. 44 we present some e^-–H_2^+ calculated differential cross sections (Chang and Temkin, 1970) for $j=0$ to 2 excitation at 6.8 eV. Of particular note is the opposite asymmetry about 90° of the singlet (σ_s) and triplet (σ_t) curves. This difference is traceable to the enhancement of the ${}^3P_{m=0}$ phase shift, for which there is no counterpart in the ${}^1P_{m=0}$ partial wave. Thus Fig. 44 offers another manifestation of the ${}^3P_{m=0}$ enhancement which was such a prominent feature of the e^-–H_2 results.

Let us summarize the contents of this section. First of all, the summarizing remarks made in the last paragraph of Sec. 3 obviously are germane. This section, like Sec. 3, certainly indicates that calculational understanding of electron–molecule scattering has progressed significantly in recent years. For the purposes of incorporating both exchange and polarization, the fixed-nuclei theory provides a reliable and convenient method of calculating the average cross section; moreover, coupled with the adiabatic-nuclei theory, it becomes an extremely effective not very arduous method for calculating most aspects of rotational excitation. However, the validity and utility of the fixed-nuclei and adiabatic-nuclei approximations must not be confused with the validity of single-center expansions, whose reliability is by no means established. Unquestionably single-center expansions do provide an approximately quantitative description; on the other hand, the degree of accuracy practicably attainable with single-center expansions is suspect, particularly for heavier diatomics. As evidence for this last assertion, in Fig. 45 we show a recent very elaborate single-center calculation of e^-–N_2 scattering, by Burke and Sinfailam (1970); Fig. 45 also sketches the data of Golden (1966a) and the theoretical curve of Fisk (1936), taken from Fig. 10. Evidently the agreement between experiment (Golden, 1966a) and the single-center Burke and Sinfailam (1970) predictions is at best qualitative. Moreover, in order for Burke and Sinfailam to obtain convergence, several terms were required in their partial-wave expansions—both for the scattered wave and for the potential. The ${}^2\Pi_g$ enhancement or shape resonance mentioned in subsec. 2.31a does show up gratifyingly in the Burke–Sinfailam calculation, but its position and height are not really correct. It appears, therefore, that spheroidal coordinates—which Hara (1969b, 1969c) was able to use practicably in his e^-–H_2 computations—will be a necessary part of accurate fixed-nuclei and adiabatic-nuclei calculations.

Adamov, M., V. Objedkov, and R. Evarestov, 1963, Litov. Fiz. Sbronik **3,** 245.
Altshuler, S., 1957, Phys. Rev. **107,** 114.
Ardill, R. W. B., and W. D. Davison, 1968, Proc. Roy. Soc. (London) **A304,** 465.
Arthurs, A. M., and A. Dalgarno, 1960, Proc. Roy. Soc. (London) **A256,** 540.
Bardsley, J. N., and M. A. Biondi, 1970, "Advan. At. Mol. Phys. **6,** 1.
——, J. N. A. Herzenberg, and F. Mandl, 1966, Proc. Phys. Soc. (London) **89,** 305.
——, J. N., and F. Mandl, 1968, *Reports on Progress in Physics,* (Institute of Physics, London), Vol. 31, Part II, p. 472.
Boness, M. J. W., and J. B. Hasted, 1966, Phys. Letters **21,** 526.
——, and G. L. Schulz, 1968, Phys. Rev. Letters **21,** 1031.
Bottcher, C., 1969, Chem. Phys. Letters **4,** 320.
——, 1970, Mol. Phys. **19,** 193.
——, 1971, Chem. Phys. Letters **9,** 57.
Bransden, B. H., and M. R. C. McDowell, 1969, J. Phys. B **2,** 1187.
Brode, R. B., 1933, Rev. Mod. Phys. **5,** 257.
Bruche, E., 1927, Ann. Physik **83,** 1065.
Burke, P. G., and S. Geltman, 1970, J. Phys. B **3,** 1062.
——, and L. T. Sinfailam, 1970, J. Phys. B **3,** 641.
——, and K. Smith, 1962, Rev. Mod. Phys. **34,** 458.
Burrow, P. D., and G. J. Schulz, 1969, Phys. Rev. **187,** 97.
Carter, C., N. March, and D. Vincent, 1958, Proc. Phys. Soc. (London) **71,** 2.
Castillejo, L., I. C. Percival, and M. J. Seaton, 1960, Proc. Roy. Soc. (London) **A254,** 259.
Chamberlain, G. E., and L. J. Kieffer, 1970, "Bibliography of Low Energy Electron Collision Cross Section Data (1967–1969)", University of Colorado, Boulder, Colorado, Joint Institute of Laboratory Astrophysics Information Center Report No. 10.
Chang, E. S., 1970, Phys. Rev. A **2,** 1403.
——, and A. Temkin, 1969, Phys. Rev. Letters **23,** 399.
——, and A. Temkin, 1970, J. Phys. Soc. Japan **29,**
Chase, D. M., 1956, Phys. Rev. **104,** 838.
Christophorou, L. G., and A. A. Christodoulides, 1969, J. Phys. B **2,** 71.
Coulson, C. A., 1938, Proc. Camb. Phil. Soc. **34,** 204.
Crawford, O. H., 1971, Mol. Phys. **20,** 585.
——, A. Dalgarno, and P. B. Hays, 1967, Mol. Phys. **13,** 181.
Crompton, R. W., 1970, *Advances in Electronics,* (Academic, New York), Vol. 2.
——, M. T. Elford, and J. Gascoigne, 1965, Aust. J. Phys. **18,** 409.
——, M. T. Elford, and R. L. Jory, 1967, Aust. J. Phys. **20,** 369.
——, D. K. Gibson, and A. I. McIntosh, 1969, Aust. J. Phys. **22,** 715.
——, D. K. Gibson, and A. G. Robertson, 1970, Phys. Rev. **A2,** 1386.
——, and A. I. McIntosh, 1968, Aust. J. Phys. **21,** 637.
Dalgarno, A., and R. J. W. Henry, 1965, Proc. Phys. Soc. (London) **85,** 679.
——, and R. J. Moffett, 1963, Proc. Natl. Acad. Sci. India **A33,** 511.
Damburg, R. J., and E. Karule, 1967, Proc. Phys. Soc. (London) **90,** 637.
Dowell, J. T., and T. E. Sharp, 1967, J. Chem. Phys. **47,** 5068.
Edmonds, A. R., 1957, *Angular Momentum in Quantum Mechanics* (Princeton U. P., Princeton, New Jersey).
Ehrhardt, H., L. Langhans, F. Linder, and H. S. Taylor, 1968, Phys. Rev. **173,** 222.
——, and F. Linder, 1968, Phys. Rev. Letters **21,** 419.
Eliezer, I., H. S. Taylor, and J. K. Williams, 1967, J. Chem. Phys. **47,** 2165.
Engelhardt, A. G., and A. V. Phelps, 1963, Phys. Rev. **131,** 2115.
——, A. V. Phelps, and C. G. Risk, 1964, Phys. Rev. **135, A1566.**
Fano, U., 1970, Phys. Rev. A **2,** 353.
Fisk, J. B., 1936, Phys. Rev. **49,** 167.
Fox, R. E., W. M. Hickam, and D. J. Grove, 1953, Phys. Rev. **89,** 555.
——, W. M. Hickam, and D. J. Grove, 1955, Rev. Sci. Instr. **26,** 1101.
——, W. M. Hickam, T. Kjeldaas, Jr., and D. J. Grove, 1951, Phys. Rev. **84,** 859.
Frost, L. S., and A. V. Phelps, 1962, Phys. Rev. **127,** 1621.
Garcia, J. D., 1967, Phys. Rev. **159,** 39.
Garrett, W. R., 1971, Mol. Phys. **20,** 751.
——, J. E. Turner, and W. V. Anderson, 1970, Oak Ridge National Laboratory Report ORNL-4431.
Geltman, S., and K. Takayanagi, 1966, Phys. Rev. **143,** 25.
Gerjuoy, E., and S. Stein, 1955a, Phys. Rev. **97,** 1671.
——, and S. Stein, 1955b, Phys. Rev. **98,** 1848.
Gilmore, F. R., 1965, J. Quant. Spectr. Radiative Transfer **5,** 369.
Golden, D. E., 1966a, Phys. Rev. Letters **17,** 847.
——, 1966b, Phys. Rev. **151,** 48.

——, and H. W. Bandel, 1965a, Phys. Rev. **138,** A14.
——, and H. W. Bandel, 1965b, Phys. Rev. Letters **14,** 1010.
——, and H. W. Bandel, 1966, Phys. Rev. **149,** 58.
——, H. W. Bandel, and J. A. Salerno, 1966, Phys. Rev. **146,** 40.
——, and H. Nakano, 1967, Bull. Am. Phys. Soc. **12,** 232.
——, and A. Zecca, 1970, Phys. Rev. A **1,** 242.
——, and A. Zecca, 1971a, Rev. Sci. Instr., **42,** 210.
——, and A. Zecca, 1971b, to be published.
Goldstein, H., 1965, "Classical Mechanics" (Addison-Wesley), pp. 107–108.
Gryzinski, M., 1965, Phys. Rev. **138,** A305, A322 and A336.
Hake, Jr., R. D., and A. V. Phelps, 1967, Phys. Rev. **158,** 70.
Hara, S., 1969a, Jour. Phys. Soc. Japan **27,** 1009.
——, 1969b, Jour. Phys. Soc. Japan **27,** 1262.
——, 1969c, Jour. Phys. Soc. Japan **27,** 1592.
Henry, R. J. W., 1970, Phys. Rev. **A2,** 1349.
——, and N. F. Lane, 1969, Phys. Rev. **183,** 221.
Henry, R. J. W., and N. F. Lane, 1971, Phys. Rev., A **4,** 410.
Herzberg, G., 1950, *Molecular Spectra and Molecular Structure I. Spectra of Diatomic Molecules* (D. Van Nostrand, Princeton, N.J.).
Hochstim, Adolf R., 1969, *Bibliography of Chemical Kinetics and Collision Processes* (Plenum, New York).
Holstein, T., 1946, Phys. Rev. **70,** 367.
Hughes, A. L., and V. Rojansky, 1929, Phys. Rev. **34,** 284.
Huxley, L. G. H., 1940, Phil. Mag. **30,** 396.
——, and R. W. Crompton, 1955, Proc. Phys. Soc. (London) **B68,** 381.
Itikawa, Y., 1967, University of Tokyo Institute of Space and Aeronautical Science Report No. 412, p. 75.
——, 1969, J. Phys. Soc. Japan **27,** 444.
——, 1970, J. Phys. Soc. Japan **28,** 1062.
——, and K. Takayanagi, 1969a, J. Phys. Soc. Japan **26,** 1254.
——, and K. Takayanagi, 1969b, J. Phys. Soc. Japan **27,** 1293.
Karl, G., and J. D. Poll, 1967, J. Chem. Phys. **46,** 2944.
Kerwin, L., P. Marmet, and J. D. Carette, 1969, "High Resolution Electron Beams and Their Application", in *Case Studies in Atomic Collision Physics I*, edited by E. W. McDaniel and M. R. C. McDowell (North-Holland Publ. Co.) Chapt. 9.
Kieffer, L. J., 1967, "Bibliography of Low Energy Electron Collision Cross Section Data", U.S. National Bureau of Standards Miscellaneous Publication 289.
Kohn, W., 1948, Phys. Rev. **74,** 1763.
Kollath, R., 1932, Ann. Physik **15,** 485.
Krauss, M., and F. Mies, 1970, Phys. Rev. **A1,** 1592.
Kuyatt, C. E., J. A. Simpson, and S. R. Mielczarek, 1964, Phys. Rev. Letters **12,** 293.
——, J. A. Simpson, and S. R. Mielczarek, 1966, J. Chem. Phys. **44,** 437.
Lane, N. F., and S. Geltman, 1967, Phys. Rev. **160,** 53.
——, and S. Geltman, 1969, Phys. Rev. **184,** 46.
——, and R. J. W. Henry, 1968, Phys. Rev. **173,** 183.
Lenard, P., 1903, Ann. Physik **12,** 714.
Linder, F., 1969, in *Abstracts of the Sixth International Conference on the Physics of Electronic and Atomic Collisions*, (M.I.T. Press, Cambridge, Massachusetts) p. 141.
Lowke, J. J., and J. H. Parker, 1969, Phys. Rev. **181,** 302.
Magnus, W., and F. Oberhettinger, 1949, *Formulas and Theorems for the Special Functions of Mathematical Physics* (Chelsea, New York), p. 149.
Margenau, H., 1946, Phys. Rev. **69,** 508.
Massey, H. S. W., and E. H. S. Burhop, 1952, *Electronic and Ionic Impact Phenomena* (Oxford U. P., Oxford, England.
——, E. H. S. Burhop, and H. B. Gilbody, 1969, "Electronic and Ionic Impact Phenomena" (Oxford U. P., Oxford, England).
——, and R. O. Ridley, 1956, Proc. Phys. Soc. (London), **A69,** 659.
McDaniel, Earl W., 1964, *Collision Phenomena in Ionized Gases* (Wiley, New York).
Mentzoni, M. H., 1965, J. Res. Natl. Bur. Std. (U.S.) **69D,** 213.
Mittleman, M., J. Peacher, and B. Rozsanyai, 1968, Phys. Rev. **176,** 180.
——, and R. E. Von Holdt, 1965, Phys. Rev. **140,** A726.
Morse, P. M., 1935, Proc. Nat. Acad. Sci. **25,** 56.
——, and W. P. Allis, 1933, Phys. Rev. **44,** 269.
——, and H. Feshbach, 1953, *Methods of Theoretical Physics* (McGraw-Hill, N.Y.), p. 1503.
Nagahara, S., 1953, J. Phys. Soc. Japan **8,** 165.
——, 1954, J. Phys. Soc. Japan **9,** 52.
Oksyuk, Y. D., 1966, Zh. Eksp. Teor. Fiz. **49,** 1261 [Soviet Phys. JETP **22,** 873.]
O'Malley, T. F., 1966, Phys. Rev. **150,** 14.
——, and H. S. Taylor, 1968, Phys. Rev. **176,** 207.
Pack, J. L., R. E. Voshall, and A. V. Phelps, 1962, Phys. Rev. **127,** 2084.
Pauling. L., and E. B. Wilson, 1935, *Introduction to Quantum Mechanics* (McGraw-Hill, New York), p. 333.
Phelps, A. V., 1967, *DASA Reaction Rate Handbook*, (General Electric Co., Missile and Space Division, Space Sciences Lab., Philadelphia, Pa.) Chap. 12 and 16.
——, 1968, Rev. Mod. Phys. **40,** 399.
Ramsauer, C., 1921, Ann. Physik **64,** 513.
——, and R. Kollath, 1930, Ann. Physik **4,** 91.
——, and R. Kollath, 1931, Ann. Physik **10,** 143.
——, and R. Kollath, 1932, Ann. Physik **12,** 529.
Rapp, D., T. E. Sharp, and D. P. Briglia, 1965, Phys. Rev. Letters **14,** 533.
Roberts, T. D., and D. S. Burch, 1966, Phys. Rev. **142,** 100.
Salop, A., and H. Nakano, 1970, Phys. Rev. A **2,** 127.
Sampson, D. H., and R. C. Mjolsness, 1965, Phys. Rev. **140,** A1466.
Schulz, G. J., 1958, Phys. Rev. **112,** 150.
——, 1959, Phys. Rev. **116,** 1141.
——, 1964, Phys. Rev. **135,** A988.
——, and R. K. Asundi, 1965, Phys. Rev. Letters **15,** 946.
——, and R. K. Asundi, 1967, Phys. Rev. **158,** 25.
——, and R. E. Fox, 1957, Phys. Rev. **106,** 1179.
Simpson, J. A., 1964, Rev. Sci. Instr. **35,** 1698.
Sloan, I. H., 1964, Proc. Roy. Soc. (London) **A281,** 151.
Smith, K. F., 1955, *Molecular Beams* (Methuen, London).
Stabler, R. C., 1963, Phys. Rev. **131,** 679.
——, 1964, Phys. Rev. **133,** A1268.
Stier, H., 1932, Z. Physik **76,** 439.
Sunshine, G., B. B. Aubrey, and B. Bederson, 1967, Phys. Rev. **154,** 1.
Takayanagi, K., 1966, J. Phys. Soc. Japan **21,** 507.
——, 1967, Progress Theor. Phys. Japan Suppl. **40,** 216.
——, 1969, "Atomic Collisions: Bibliography No. 8, Electron Collisions with Atoms and Molecules (Experimental) Part I (1921–1960)", distributed by the University of Tokyo Institute of Space and Aeronautical Science.
——, and Y. Itikawa, 1968, J. Phys. Soc. Japan **24,** 160.
——, and Y. Itikawa, 1970, Advan. At. Mol. Phys. **6,** 105.
Tate, J. T., and P. T. Smith, 1932, Phys. Rev. **39,** 270.
Taylor, H. S., and J. K. Williams, 1965, J. Chem. Phys. **42,** 4063.
Temkin, A., 1957, Phys. Rev. **107,** 1004.
——, and F. Faisal, 1971, Phys. Rev. A **3,** 520.
——, and J. C. Lamkin, 1961, Phys. Rev. **121,** 788.
——, and K. V. Vasavada, 1967, Phys. Rev. **160,** 109.
——, K. Vasavada, E. Chang, and A. Silver, 1969, Phys. Rev. **186,** 57.
Thomson, J. J., 1912, Phil. Mag. **23,** 449.
Townsend, J. S., 1914, *Electricity in Gases* (Oxford U. P., Oxford, England).
——, and V. A. Bailey, 1922, Phil. Mag. **44,** 1033.
Tully, J. C., and R. S. Berry, 1969, J. Chem. Phys. **51,** 2056.
Turner, J. E., V. E. Anderson, and K. Fox, 1968, Phys. Rev. **174,** 81.
Varney, R. N., and L. H. Fisher, 1968, Methods Exper. Phys. **7** Part B, 29.
Veatch, G. E., J. T. Verdeyen, and J. H. Cahn, 1966, Bull. Am. Phys. Soc. **11,** 496.
Vriens, L., 1969, "Binary Encounter and Classical Collision Theories", in *Case Studies in Atomic Collision Physics I*, edited by E. W. McDaniel and M. R. C. McDowell (North-Holland Publ. Co.), Chapt. 6.
Wang, S. C., 1928, Phys. Rev. **31,** 579.
Weingartshofer, A., H. Ehrhardt, V. Hermann, and F. Linder, 1970, Phys. Rev. **A2,** 294.
Wilkins, R. L., and H. S. Taylor, 1967, J. Chem. Phys. **47,** 3532.